SANDIA REPORT

SAND2003-3407
Unlimited Release
Printed December 2003

The Disturbed Rock Zone at the Waste Isolation Pilot Plant

Francis D. Hansen

Prepared by
Sandia National Laboratories
Albuquerque, New Mexico 87185 and Livermore, California 94550

Sandia is a multiprogram laboratory operated by Sandia Corporation,
a Lockheed Martin Company, for the United States Department of Energy's
National Nuclear Security Administration under Contract DE-AC04-94AL85000.

Sandia National Laboratories

Issued by Sandia National Laboratories, operated for the United States Department of Energy by Sandia Corporation.

Available to DOE and DOE contractors from
U.S. Department of Energy
Office of Scientific and Technical Information
P.O. Box 62
Oak Ridge, TN 37831

Telephone: (865)576-8401
Facsimile: (865)576-5728
E-Mail: reports@adonis.osti.gov
Online ordering: http://www.doe.gov/bridge

Available to the public from
U.S. Department of Commerce
National Technical Information Service
5285 Port Royal Rd
Springfield, VA 22161

Telephone: (800)553-6847
Facsimile: (703)605-6900
E-Mail: orders@ntis.fedworld.gov
Online order: http://www.ntis.gov/help/ordermethods.asp?loc=7-4-0#online

SAND2003-3407
Unlimited Release
Printed December 2003

The Disturbed Rock Zone at the Waste Isolation Pilot Plant

Francis D. Hansen
Carlsbad Programs Group
Sandia National Laboratories
P.O. Box 5800
Albuquerque, NM 87185-1395

Abstract

The Disturbed Rock Zone constitutes an important geomechanical element of the Waste Isolation Pilot Plant. The science and engineering underpinning the disturbed rock zone provide the basis for evaluating ongoing operational issues and their impact on performance assessment. Contemporary treatment of the disturbed rock zone applied to the evaluation of the panel closure system and to a new mining horizon improves the level of detail and quantitative elements associated with a damaged zone surrounding the repository openings. Technical advancement has been realized by virtue of ongoing experimental investigations and international collaboration. The initial portion of this document discusses the disturbed rock zone relative to operational issues pertaining to re-certification of the repository. The remaining sections summarize and document theoretical and experimental advances that quantify characteristics of the disturbed rock zone as applied to nuclear waste repositories in salt.

Contents

1.0 Introduction .....

2.0 Option D Modeling .....

2.2 Background of Option D Panel Closure Analyses 10

2.3 Option D in the Technical Baseline Migration 11

2.4 Preliminary Option D Assessment 16

3.0 Clay G Evaluations .....

3.1 Background of Clay G Analyses 17

3.2 Results of Clay G Analysis 19

3.3 Conclusions of Clay G Analyses 23

4.0 Salt Damage Evaluations .....

4.1 Principles of Salt Damage 25

4.2 Hydrologic Properties of Damaged Salt 26

4.3 Laboratory Studies of Salt Damage 27

4.4 Salt Damage Modeling 30

4.5 Salt Damage Healing in Laboratory Studies 31

4.6 Salt Damage Healing—*In Situ* Small Scale 32

4.7 DRZ Delineation by Sonic Velocity 33

4.8 Observational Fracture Studies 36

4.9 Full-Scale Field Analogs 39

5.0 Summary .....

6.0 References .....

LIST OF TABLES

Table 1. DRZ Permeability used in the CCA and PAVT 9
Table A.1 Summary of Strength and Permeability Tests on 51

LIST OF FIGURES

Figure 1. Detail of PAVT and TBM grid and properties 12
Figure 2. Damage in the Floor of Panel 1, Room 2, August 21, 2001 13
Figure 3. Stratigraphy near the Repository Horizon (after Kreig, 1984) 14
Figure 4. Schematic of the Stratigraphy Surrounding the Raised and Unraised Sections of the Repository 15
Figure 5. En Echelon DRZ Fracture Pattern to Clay G 19
Figure 6. Porosity Histories for Raised and Original Horizons Using Various Gas Generation Parameters 20
Figure 7: Deformation of Raised Disposal Room Containing Waste with Time for *f*=0.0 21
Figure 8: Anhydrite Shear Failure around the Raised Disposal Room with Time for *f*=0.0 22
Figure 9: Disturbed Rock Zone around a Raised Disposal Room with Time for f=0.0 23
Figure 10. Stress States Known to Cause Dilation of WIPP Salt 29
Figure 11. Permeability Versus Dilatant Volumetric Strain for WIPP Salt 30
Figure 12. Damage Predicted Around a Typical WIPP Disposal Room 40 Years After Excavation (after Van Sambeek et al., 1993b) 31
Figure 13. Layout of Holes for Room Q Alcove, with holes used for ultrasound measurements indicated in red 34
Figure 14. Same-hole measurements for adjacent holes, one in the left-hand wall (red) and in the corner (black) 35
Figure 15. Fractures and Apertures in Three WIPP Cores 38
Figure 16. Fracture Apertures for DRZ Cores from WIPP and Asse 39
Figure 17. ALOHA2: Permeability Distribution around the Bulkhead and Open Drift 40
Figure A.1. Permeability of SMC, ESC, and MSC Concrete Specimens Versus Gas Pressure Difference 52
Figure A.2. Cumulative Distribution Function for Permeability of SMC (after Repository Isolation Systems Department, 1996, WIPP Shaft Seal System Compliance Submittal Design Report, Appendix A) 53

1.0 Introduction

The Disturbed Rock Zone (DRZ) is an important geomechanical element of the Waste Isolation Pilot Plant (WIPP). The DRZ was modeled explicitly in the Compliance Certification Application (CCA) and in the Performance Assessment Verification Test (PAVT). On the basis of the performance calculations, WIPP was certified by the U.S. Environmental Protection Agency (EPA) as meeting regulatory compliance. Since the certification, the scientific understanding of the DRZ has progressed by virtue of ongoing experimental investigations, further evaluations of published research, and international collaborations. This paper reviews the considerable information base on the DRZ and contrasts today's understanding with the representation utilized for the compliance determination. As documented subsequently, DRZ properties are bracketed more definitively today than at the time of the compliance certification application, thereby making it possible to represent elements of the underground in a more realistic manner than represented heretofore.

To begin the evaluation of the current WIPP operational framework in which DRZ issues are addressed, a limited discussion of DRZ evolution helps set the stage. The WIPP is situated in primarily rock salt at a depth of 655 meters. Salt, being a plastic medium at this depth, exhibits a virgin lithostatic state of stress. Creation of underground openings perturbs the static equilibrium of the mined regions sufficiently to cause fracturing in rock proximal to the extracted material. The DRZ comprises the region near an excavation that experiences a change in hydrologic or mechanical properties. The properties that typically define a DRZ include: (1) dilational deformation ranging from microscopic to readily visible scales, (2) loss of strength evidenced by rib spall, floor heave, roof degradation and collapse, and (3) increased fluid permeability via connected porosity. The DRZ can play an important role in the geomechanical response of the WIPP underground, particularly where structures are placed to retard fluid flow in the repository. Although stress differences tend to decrease over time in a creeping medium, such as rock salt, fractures continue to grow and coalesce in an arching pattern around drifts and develop preferentially oriented parallel to the opening. As shown in photographs later in this report, the manifestation of the DRZ can be observed today in several locations in the WIPP underground.

Treatment of the DRZ is integral to the evaluation of two features of the operating repository that have changed relative to the analyses supporting the initial certification:

- The Option D panel closure to be implemented as a condition of the certification, and,
- The operational change elevating the repository disposal room ceiling to Clay Seam G.

These two considerations, which involve several geomechanical elements, will be referred to as Option D and Clay Seam G, respectively. In particular, construction of Option D will create conditions substantially different from those modeled in the compliance calculations. Namely, the salt DRZ would heal around such a rigid monolith and the anhydrite comprising Marker Bed 139, a major component of the DRZ, beneath the current repository floor would be mined out. Raising the repository horizon by 2.43 meters to Clay G changes the structural setting by increasing the thickness of salt in the floor between the repository and MB 139 and decreasing the distance from the roof to overlying marker beds, such as Marker Bed 138. Construction of Option D within the raised repository setting is not addressed at this time.

The primary motivation for developing this paper derives from the need to incorporate these two features in structural analysis of the underground setting and implement the derivative information into PA analyses. The EPA certified WIPP compliance previously; however, incorporation of these operational features necessitated conceptual model modifications and additional detail to the PA models. In anticipation of the scrutiny associated with re-certification, the geotechnical aspects of Option D and Clay Seam G features are evaluated to ascertain deviations from the certified baseline. Technical documentation demonstrates and substantiates that these two changes can be adequately represented and understood and that they do not perceptibly change the PA cumulative complementary distribution function. In addition to evaluating these operational details, the broader context of a damaged rock in a salt repository will be reviewed and updated to include recent work at WIPP and within international repository programs.

In preparation for the compliance re-certification application, a prerequisite to the EPA deliberations includes assessment of advances in our knowledge of features, events and processes pertaining to WIPP. In technical exchanges between the DOE, EPA and stakeholders during the period between the compliance determination and the re-certification application, ongoing technical assessment of the DRZ was discussed periodically. Technical understanding of the DRZ has been recorded in reference literature, such as external publications, SAND documents published by Sandia National Laboratories, and biannual progress reports on repository investigations. This document emphasizes present advances with respect to quantifying characteristics of the DRZ and provides a literature review, both of which emphasize WIPP applications. This document is meant to provide comprehensive documentation and technical discussion of the DRZ relative to WIPP re-certification. In particular, the technical discourse emphasizes improvement to our understanding of the DRZ at WIPP.

This document provides a review and assessment of the Project's understanding of the WIPP DRZ. Liberal reference will be made to a large amount of available information. The layout of this paper is an attempt to be comprehensive and systematic. Flow of the content begins with background information, which contrasts previous and current treatment of the DRZ in performance assessment analyses. Then, treatment of the two primary features—Option D and Clay G—will be addressed in Sections 2 and 3, respectively. Section 4 presents an overview of characteristics of the DRZ, which substantiate many of the parameters and modeling treatment of the DRZ. Section 4 reviews underlying theory and characteristics of the DRZ, and provides a summary updating the understanding of the DRZ. The emphasis of the new treatment is the DRZ itself, particularly the "salt" DRZ, but other elements of the underground, such as the concrete of Option D and fracture of the anhydrite, are involved in the analyses. These geomechanical elements as represented in the baseline compliance calculations and subsequent PA verification testing have been updated for re-certification calculations. The updated implementation is believed to represent an improvement in accuracy, adequacy and validity of the modeling employed for the initial certification.

2.0 Option D Modeling

The PA calculation was conducted in 1996 (U.S. DOE, 1996) as part of the overall compliance certification process established by the EPA in its radiation protection regulations (U.S. EPA,

1998). In 1997 the EPA required a PAVT to verify and evaluate the results of DOE's CCA PA calculation. In their analysis, EPA addressed DRZ parameter values and distributions. To support the upcoming re-certification process, the technical baseline of the CCA and the PAVT was converged.

The table below summarizes the DRZ parameter changes made between the CCA and the PAVT. The grid used in CCA calculations implemented a DRZ of constant permeability (10^{-15} m^2) over a region 12 meters above and 2.23 meters below the disposal rooms. The grid was continuous above panel closure systems, such that the same permeability and thickness existed above and below the simulated panel closures. The PAVT changed the DRZ permeability to a uniform distribution ranging from $10^{-19.4}$ to $10^{-12.5}$ m^2. The geometrical dimensions of the DRZ are the same between the CCA and the PAVT. A consensus was reached that the PAVT permeability values represented an acceptable range for purposes of those analyses and assumptions pertaining thereto. Sandia National Laboratories reconciled all the parameters used in the CCA and the PAVT and established a single parameter baseline for the compliance re-certification calculations (Hansen and Leigh, 2002).

Table 1. DRZ Permeability used in the CCA and PAVT.

DRZ Permeability Material ID's	CCA Value	Description of Change for the PAVT	Rationale
198 - DRZ_1/prmx_log 199 - DRZ_1/prmy_log 200 - DRZ_1/prmz_log	-15	Log of the DRZ permeability (m^2) was changed to a uniform distribution ranging from -19.4 to -12.5.	Based on gas permeability testing of anhydrite cores from MB 139 (see WPO #30603 p. 2; WPO #32038; WPO #38367 p. 11)

The EPA documented their reasons for selecting PAVT DRZ permeability distributions, which differed from the single permeability value used in CCA calculations. Records from the WIPP Project Office (WPO) were used by the EPA to derive the recommended PAVT permeability range, which includes the CCA value near the mid-range of PAVT distribution. The WPO records are listed in the table. Additional documentation is cited in Sandia National Laboratories electronic database (PRAMVIEW). The DRZ parameters now assembled in PRAMVIEW are those selected by the EPA for the PAVT.

A brief review of the WPO documents supporting the PAVT DRZ values supports the magnitude and range of the PAVT values. WPO #32038 includes one data set comprising 14 tests, which yields a permeability range (log 10) from –12.5 to –21 m^2. The other two WPO packages noted in the table include laboratory measurements on Marker Bed 139 anhydrite. From a total of 42 anhydrite samples, a pressure-sensitive permeability from (log 10) –16 to –21 m^2 was reported. Based on these data the range employed by the PAVT is appropriate.

The CCA and PAVT are documented, extensive, complicated calculations, which underpin the compliance determination. In addition, the "record" includes reference documents of many types, such as Technical Support Documents (TSDs), and Compliance Application Review Documents (CARDS). These records were scrutinized for their applicability to the DRZ model.

A summary of the review of technical discussions existing in the records is included in this report (Appendix B).

2.2 Background of Option D Panel Closure Analyses

In terms of PA, the most important DRZ parameters are permeability, porosity, and their extent. In the period since the compliance application, WIPP personnel have re-examined the DRZ model, paying particular attention to implementation of Option D panel closure systems. Analysis Plan 087 (Hansen et al., 2002) describes the incorporation of the Option D closure into the existing BRAGFLO grid. The migration from the initial representations of the closures and DRZ to a more detailed analysis was called a Technical Baseline Migration (TBM). Detail is added to simulate more closely the actual geometry of the WIPP underground. Permeability is a primary modeling parameter, therefore a contrast will be drawn between treatment of the DRZ for compliance certification calculations, PA verification test calculations, and more recent calculations performed to reconcile parameters, representations and conceptual models into a single baseline. The primary motivation to add detail to the BRAGFLO grid is to incorporate a more realistic representation of the geotechnical issues attendant to Option D.

Implementation of Option D into the PA model necessitated additional detail within the BRAGFLO mesh to capture the geotechnical interplay between the DRZ, the anhydrite marker beds and the concrete monolith. The salt DRZ and the marker bed response are also integral to interpretation of the effects caused by raising the disposal horizon (see Section 3.0). Perspectives, background, and data will be provided to guide the arguments toward the analysis being undertaken to evaluate incorporation of Option D panel closures into the PA calculations. Calculations underway for re-certification refine the detail of the repository and evaluate effects of the DRZ in concert with the panel closure Option D.

Permeability values and geometrical extent of the DRZ are based on observations, measurements and an understanding of the mechanical response. The DRZ is also reversible in salt. When a rigid plug, such as the Option D panel closure concrete, is placed in a drift, the impinging salt experiences a "back-stress", which reduces stress differences. As the state of stress approaches equilibrium, existing microfractures heal within the salt medium. Thus, the expectation is that the DRZ around an Option D panel closure would be minimal at the time of construction and eliminated essentially immediately after the panel closure is completed. By contrast, the DRZ around rooms filled with waste would continue to evolve as the country rock deforms into the open space of the room and then compresses the waste stack. In a relatively short time (fewer than 100 years), however, the state of stress in the salt around the waste rooms will return to their original condition of no shear, and the DRZ around the greater areas of the waste rooms would be largely healed as well. Implications of DRZ healing and the underlying theory are discussed in Section 4.

Placement of a rigid structure within a drift, such as provided by the Option D concrete monolith, will resist the inward flow of salt and locally return the state of stress to a condition that no longer produces a DRZ, rather conditions would favor healing of damaged salt. In addition, the DRZ is excavated prior to placement of the concrete structure. Therefore, consideration of the

model for an Option D panel closure must include properties of the structure placed in the drift, particularly its permeability, and properties of the surrounding rock. Characteristics of the Salado Mass Concrete (SMC) specified for the Option D closure are summarized in Appendix A.

In the course of WIPP analyses, the DRZ proximal to the disposal rooms and extending into panel entry drifts has been (and is proposed to be) represented in the following ways.

DRZ and panel closure in the CCA.

- DRZ permeability was held constant at 10^{-15} m^2.
- The DRZ extended 12 meters above and approximately 2 meters below (bottom of Marker Bed 139).
- The panel closure was represented with a permeability of 10^{-15} m^2.
- Anhydrite fracture occurred when gas pressure approached lithostatic.

DRZ and panel closure in the PAVT.

- DRZ permeability was sampled from $10^{-19.4}$ to $10^{-12.5}$ m^2 with a median permeability of $10^{-15.95}$ m^2.
- The DRZ extended 12 meters above and approximately 2 meters below (bottom of Marker Bed 139).
- The panel closure was represented with a permeability of 10^{-15} m^2.
- The pressure-induced fracture model (designed for the anhydrite marker beds) was applied to the DRZ.

DRZ and panel closure in the TBM

- The PAVT permeability distribution was applied to the vast majority of the DRZ.
- The DRZ extended 12 meters above and approximately 2 meters below the disposal rooms, however the DRZ residing above and below placement of the Option D concrete monolith assumed a low permeability.
- The panel closure concrete was represented with an appropriate permeability distribution (10^{-17} to 10^{-21} m^2), as discussed in Appendix A.
- The pressure-dependent fracture model was applied to the DRZ. Conceptually, fluid could access anhydrite marker beds and allow migration around the panel closure through Marker Bed 139 or propagate into overlying anhydrite seams, which are underlain by thin clay seams.

2.3 Option D in the Technical Baseline Migration

To implement the various details required to model Option D and to prepare analyses for review by independent technical peers, Sandia embarked on an exercise called the TBM. The TBM grid refinement represented Option D closures with SMC, the DRZ above and below disposal rooms, and the DRZ above and below the Option D closure. SMC is Portland-cement concrete that is saturated with respect to NaCl (see Appendix A). Anhydrite characteristics remain the same as used in PAVT. Elements of the panel closure system are interrelated. For example, the evolution of the DRZ is a function of stress state, which changes as salt creep redistributes the superincumbent loading. A rigid concrete monolith further affects the state of stress, which rapidly decreases the deviatoric stress component and approaches equilibrium. Therefore,

appropriate parameter selection must include the coupled system. The sketches in Figure 1 illustrate the differences between the PAVT and the TBM grid. The accompanying parameters provide explicit refinement to capture detail of the Option D panel closure systems that is not represented in the PAVT.

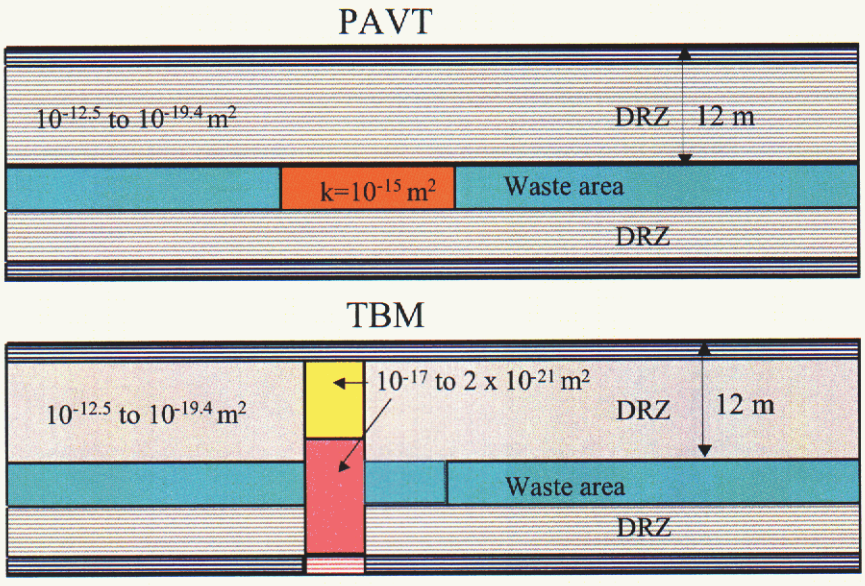

Figure 1. Detail of PAVT and TBM grid and properties.

Some fundamental issues with respect to treatment of the DRZ were addressed as the models and grid were changed to accommodate the details that Option D introduced. Analyses Plan AP-106 (Stein and Zelinski, 2003) defined the strategy. Some of the deliberations are reviewed here. Previous analyses in the PAVT allowed fracture in the upper salt DRZ to provide a gas pathway for high repository pressures. Thereby, the PAVT analysis did not yield unrealistically high pressures in the repository. It is equally probable that the floor DRZ would allow flow to Marker Bed 139, which resides 1.4 meters below the repository horizon. Marker Bed 139 comprises a nominally 1-m anhydrite layer that would not be expected to heal in the same manner as salt when it is damaged. Fractures around existing openings, such as shown in the photograph in Figure 2, evidence the nature of the damage in the floor of the repository. Extensive floor heave was observed as rooms in Panel 1 were reshaped to the original 4X10 meter rectangular cross section. Approximately one meter of the floor was removed to re-establish the original height of 4 meters. Given the extensive damage in the floor and that the rock comprises anhydrite, it is probable that brine or gas flow to Marker Bed 139 is possible when high pressure is modeled in the repository.

Figure 2. Damage in the Floor of Panel 1, Room 2, August 21, 2001.

The situation gets a little more complicated when the repository horizon is raised 2.4 meters to Clay Seam G. In the raised half of the repository, the distance through the lower DRZ from the repository floor downward to Marker Bed 139 will increase from 1.4 meters to approximately 3.8 meters. This change means that fracturing associated with floor heave will likely be reduced in the raised part of the repository. The raised waste rooms will have ready access to the Anhydrite "b" layer, which would now be excavated at the crown line of the raised waste rooms. Anhydrite "b" is a thin (~6 cm-thick), layer that is present directly above Clay Seam G, as the stratigraphy near the repository illustrates in Figure 3. Because of the availability and likely connectivity to anhydrite seams both above and below the repository horizon, it was deemed appropriate to model potential fluid flow in both the upper and lower DRZ. In the event of high repository pressures it is equally likely that a fracture pathway would form (1) parallel to the roof of the repository via Anhydrite "b", (2) vertically through the 2 m-thick DRZ to Anhydrite A--associated with Clay H, or, (3) into the floor to Marker Bed 139.

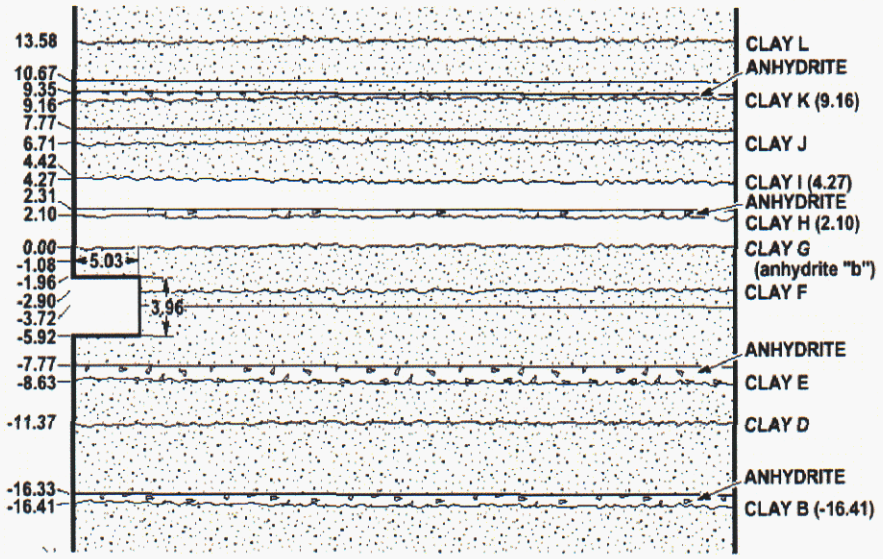

Figure 3. Stratigraphy near the Repository Horizon (after Kreig, 1984).

The phenomenon of high-pressure opening of fractures can be envisioned as hydrofractures that tend to open preferentially normal to the direction of the minimum principal stress. To examine hydrofracture in more detail, field studies (Wawersik and Stone, 1989) were re-evaluated. The results of hydraulic fracturing tests performed in WIPP salt, 3 to 100 meters from excavated rooms indicate that the pressures at which hydraulic fracturing is initiated, fall in the same range as hydrofracture tests performed in anhydrite Marker Beds 139 and 140 (Wawersik et al., 1997). Fracture initiation pressures for the anhydrite tests ranged from 7.36 to 12.46 MPa with an average initiation pressure of 10.5 MPa. Fracture initiation pressures for the salt tests ranged from 4.14 to 17.24 MPa with an average initiation pressure of 11.98 MPa (Wawersik and Stone, 1989). One important difference in the fracture behavior of intact salt is that because it is so impermeable, fractures in WIPP salt will tend to stop at more permeable anhydrite marker beds and change direction, moving along the bed rather than fracturing across beds (Wawersik et al., 1997). These data indicate that fractures in both materials will typically initiate at pressures below lithostatic and thus repository pressures significantly above lithostatic are unjustified and unexpected.

Because the data support the application of the fracture model to intact salt in addition to the marker beds, calculations incorporated fracturing in both the upper and lower DRZ. Even in the parts of the repository that are not being raised to Clay Seam G, the test results support implementing the fracture model to both the upper and lower DRZ, considering the inherent uncertainty in exactly how the system will behave under possible near-lithostatic stresses. The important process that the fracture model simulates is the bleed off of very high pressures. Whether these pressures bleed off through the upper or lower DRZ is not the salient point; rather, the important modeling process is one of pressure relief. The parameters used by the BRAGFLO fracture model and applied to the marker beds and the DRZ are justified, because they do not allow repository pressures to exceed lithostatic pressure significantly.

Figure 4 compares the raised and unraised repository configurations in relation to the surrounding stratigraphy. In the grid used for compliance re-certification, regions where the Option D panel closures intersect a marker bed are treated as isolated blocks of marker bed material. This representation is warranted for two reasons. First, the marker bed material has a very similar permeability distribution (10^{-21} to 10^{-17} m^2) as the concrete portion of the Option D panel closures. Second, in the case of high pressures (near lithostatic) it is expected that fracturing may occur in the anhydrite marker beds and flow could go "around" the panel closures out of the 2-D plane considered in the model grid. In this case the flow would be through the marker bed material that is already allowed to fracture in the model. Therefore, treating these isolated cells as anhydrite marker bed material is appropriate.

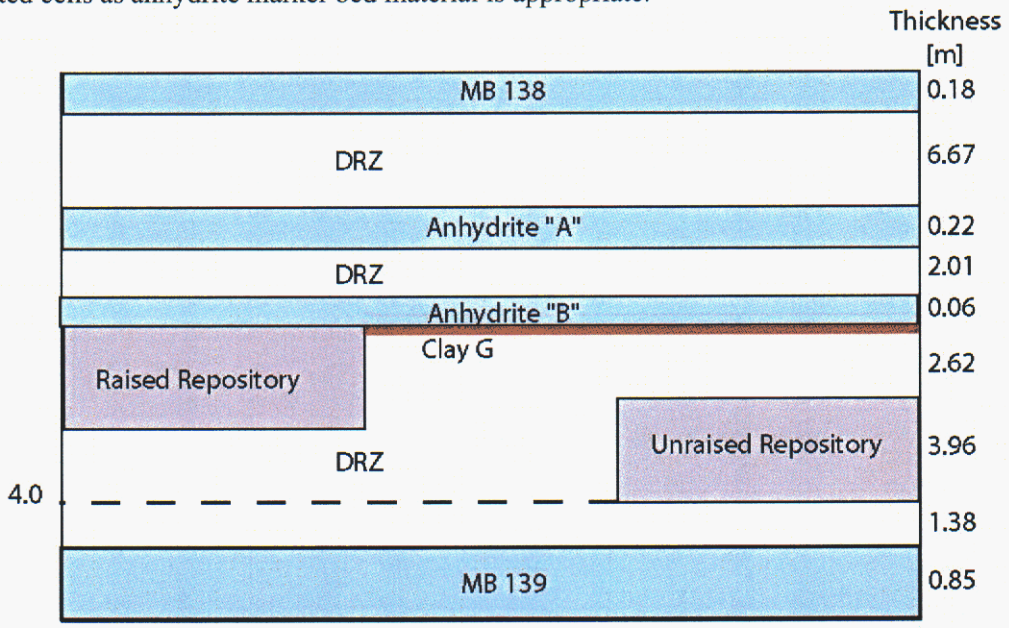

Figure 4. Schematic of the Stratigraphy Surrounding the Raised and Unraised Sections of the Repository. Not to scale. (Stein and Zelinski, 2003)

One purpose of the grid change is to incorporate appropriate detail to represent Option D panel closures more accurately than either the CCA or the PAVT. As shown in Figure 1, the PAVT grid did not include detail associated with Option D, such as the mining to remove the local DRZ. The Option D panel closure system calls for removal of DRZ around the circumference of the panel entry, and removes anhydrite Marker Bed 139 in the floor, as illustrated by the TBM grid shown in Figure 1. Details incorporated in the re-certification calculations include DRZ permeability as depicted and permeability values of the SMC, a salt-based concrete included as part of the condition for Option D. Properties used for the salt-based concrete are summarized in Appendix A.

Calculations implementing the refined grid were conducted to the point of assessing the repository saturations and pressures over the regulatory period of 10,000 years. When detail was

added for the Option D elements, a complex variation of the pressures and saturations was observed. These calculations and the underlying modeling rationale were provided to an independent peer review panel, which was empanelled consistent with requirements of Title 40 Code of Federal Regulations (CFR) 1297. The peer review panel's assessment of these conceptual model changes are summarized in Section 2.4.

2.4 Preliminary Option D Assessment

During the spring of 2002, the DOE directed Sandia to make a preliminary calculation whereby Option D was modeled within the PAVT grid simply as a relatively tight plug. This preliminary assessment helped kick-start a re-design of the panel closure system. Results were provided to CBFO (Hansen, 2002). Assessing the impact of an Option D panel closures on repository performance was challenging because the CCA and the PAVT comprise the regulatory baseline for WIPP certification. However, neither the CCA nor the PAVT explicitly represented Option D panel closures in the calculations. To provide a baseline for assessing the effects of changing the panel closure design, the DOE felt a PA that included Option D panel closures must be completed and that the accepted PAVT grid be used.

This assessment explicitly represented the Option D panel closures in the EPA-approved models of the repository, using the computational grid and parameter values that were used for the PAVT. However, the PAVT grid may be insufficiently detailed to capture all the important effects of the Option D panel closures. Subsequently Sandia conducted a second PA in which the computational grid was revised to represent the panel closures more realistically. A comparison was made between the repository performance with the Option D panel closures and the repository performance as calculated using the PAVT grid. In general, results indicate that panel closure characteristics are unlikely to affect repository performance significantly.

Peer review of conceptual models developed by the DOE for the WIPP is required by Title 40 CFR 194.27. To meet this requirement, the CBFO conducted a peer review of the three conceptual models that were changed in response to the Option D requirement and to incorporate knowledge gained since the original conceptual models were developed. The peer review panel examined the following conceptual models and their implementation:

- Disposal System Geometry
- Repository Fluid Flow, and
- DRZ.

The peer review process is a documented, critical review performed by peers who possess qualifications at least equal to those of the individuals who conducted the original work and independent of the work being done (Caporuscio et al., 2003). In most of their considerations the peer panel assessed the proposed changes against the existing implementation in the CCA or the PAVT. The panel concluded that the technical migration implemented for Option D was reasonable and adequate as summarized from their report below:

Disposal System Geometry. With respect to the disposal system geometry, the system characterized by the Option D concrete monolith and the explosion wall led to proposed change in the grid geometry since the existing grid block discretization was perceived to be too coarse for the representation of the specifics of Option D and the interrelated impacts on the DRZ. The

panel concluded that the geometry retains the features of the original conceptual model and grid changes appear reasonable and sound.

Repository Fluid Flow. The panel also determined that the repository fluid flow conceptual model was both reasonable and adequate for its intended purpose.

Disturbed Rock Zone. The panel stated that the DRZ model represents a reasonable development of the earlier alternatives. The methods and procedures used in the changed model are refinements of the previous models, and modulate the relationship between repository pressure, waste degradation and brine inflow in a more realistic and conservative way than preexisting models, while integrating the influences of two design changes. The panel's perception that excavation to Clay G is not a significant change in concept will be explored in the following Section 3.

3.0 Clay G Evaluations

This section summarizes a series of structural calculations executed to examine possible effects of raising the WIPP repository horizon from the original design level upward 2.43 meters. These calculations allow evaluations to be made of various features involved with the conceptual models implemented in WIPP PA. Notably this work addresses issues raised in an EPA letter to Carlsbad Field Office dated August 6, 2002. In the subject letter the EPA stated "*the conceptual model for the repository should reflect the change to raise the level of excavation to clay seam G. The conceptual change should be appropriately addressed in the modeling, if warranted*" (U.S. EPA, 2002). The Clay Seam G analyses included significant efforts to qualify the finite element code SANTOS. The primary results involve the production of porosity surfaces for PA. These computations also allow evaluation of the DRZ behavior and anhydrite fracture. The calculations support the modeling concepts used for the disposal area rock mechanics. In addition, details of the geomechanical structural elements provide examples of appropriate treatment of these features in PA.

3.1 Background of Clay G Analyses

Clay Seam G structural evaluations began with qualification of the finite element code SANTOS, the finite element code used for calculations supporting the original compliance certification porosity surface. At the time of the CCA, this code was executed on a Cray J916 machine. For the current analyses of Clay G the code was run on a Linux P4 Intel workstation. The first step in the requisite analyses was to replicate the CCA calculation of the porosity surface. These calculations verified that identical results can be obtained today, despite use of a new computational platform. Concomitantly, the verification and validation test problems were run to verify SANTOS functionality.

The structural analysis models repository behavior of waste-filled disposal rooms raised 2.43 meters above the present, or original, repository level. The DRZ evolution comprises a fundamental component of this analysis. The goal of these analyses is to assess whether or not raising the repository to Clay Seam G has any significant impact on the conceptual models used

in PA. Results of these analyses provides an opportunity to review treatment of the DRZ within the context of WIPP.

The analysis period is 10,000 years after waste emplacement. The calculations include mechanical creep closure response of a filled disposal room in a manner employed for baseline calculations supporting the compliance application. These calculations included construction of the three-dimensional porosity surfaces used for WIPP PA activities (Park and Holland, 2003). Thus, the primary output of Clay G structural calculation pertains to development of the porosity surface for PA.

The WIPP management and operating contractor, Washington TRU Solutions (WTS), gained concurrence of the DOE and EPA to raise the disposal room 2.43 meters above the present level. The elevation change means the roof of a disposal room would coincide with the Clay Seam G horizon and the floor would be separated from the underlying Marker Bed 139 by 3.81 meters instead of 1.38 meters (the existing separation in disposal Panels 1 and 2). The change in repository horizon was recommended to ease ground control conditions. Fractures surrounding the existing horizon tend to coalesce in an arch, which mimics the shear stress trajectories. These patterns can be seen in the underground today where the roof has been taken down along the length of the East 140 drift (see Figure 5). The roof rock of the original horizon tends to de-couple at Clay G, as exhibited by the shear fracture patterns. Underground operations personnel are currently obligated to provide roof support and maintenance that they believe would be minimized if the roof of the disposal rooms is raised to Clay G. Raising the repository disposal horizon presents a different combination of lithologies intimate to the disposal room than that of the compliance baseline. Thus, it is necessary to evaluate the impact of this proposed mining change.

Figure 5. En Echelon DRZ Fracture Pattern to Clay G.

The analysis replicated results reported in "Final Disposal Room Structural Response Calculations, SAND97-0795" (Stone, C.M., 1997), which is the referenced baseline report for the CCA. Calculation procedures and data of SAND97-0795 were used in this analysis and the results of a new, current analysis were compared with the results of SAND97-0795. Therefore, the initial calculations replicate room pressure and porosity histories for various gas generation rates for a period of 10,000 years following excavation and waste emplacement.

3.2 Results of Clay G Analysis

A recent report authored by Park and Holland (2003) provides the comprehensive results of these structural analyses. A few notable examples of the analyses are provided here, with an emphasis given to the DRZ implications. First the porosity histories for future states of the repository were replicated as shown in Figure 6. This figure plots porosity over time for representative gas generation factors and superimposes Clay Seam G results over the results obtained for the original repository horizon. In detail, many such calculations were executed to obtain porosity surfaces, but this example illustrates both replication of the previous results underpinning the CCA and the slight influence on these results that raising the repository horizon imparts to these baseline results. The CCA grid and material properties were run and results overlay previous calculations by Stone (1997). Then the grid was modified slightly to reflect elevation of the

repository horizon by 2.43 m, and the model was re-executed. Recall that the Stone calculations included gas generation with rates imposed by a factor *f*. In Figure 6 the Stone porosity results are reproduced for gas generation factors of 0.0 and 0.5. A comparison is made to the porosity results derived from the new horizon at 2.43 meters upward. In terms of room closure operating in concert with gas generation, Figure 6 demonstrates that the porosity surface for the upper horizon is identical, for all practical purposes, to the baseline porosity surface.

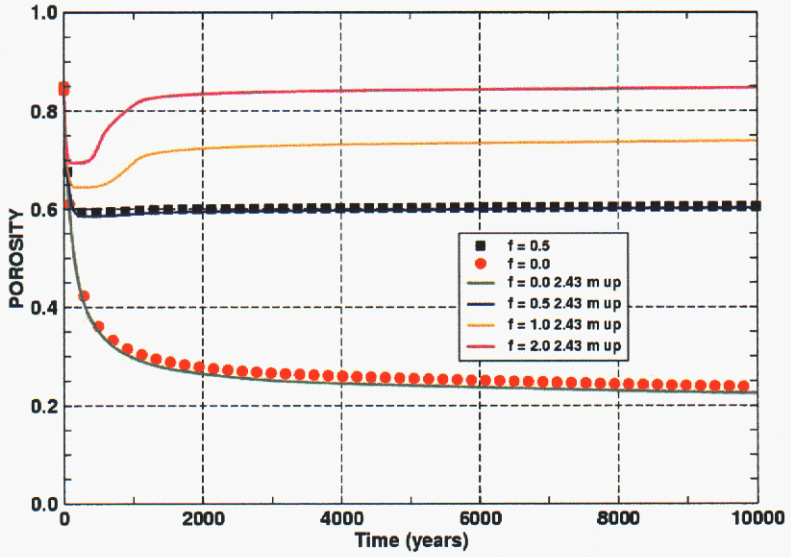

Figure 6. Porosity Histories for Raised and Original Horizons Using Various Gas Generation Parameters,.

The next series of figures illustrates representative geomechanical results from Park and Holland (2003). In Figure 7 the original grid and deformation over time are shown for the future without gas generation. The deformed mesh helps clarify the physical extent of deformation. Over time the surrounding salt deforms over 2 meters into the disposal room compressing the waste inside. The anhydrite layers are dragged along with the salt, thus ensuring extensive fracturing within these marker beds. Figure 8 focuses on the anhydrite layers themselves, and shows the state of stress easily exceeds a Drucker-Prager failure criterion. Note the MSF represents the material safety factor, which compares the existing state of stress to the Drucker-Prager criterion and MSF>1 denotes failure. Also note in Figure 8 that the state of stress difference would decrease over time and less of the anhydrite would reside in failed stress space. Whereas salt has been shown to heal as the stress state approaches equilibrium (reducing deviatoric stress), anhydrite has not demonstrated similar healing characteristics.

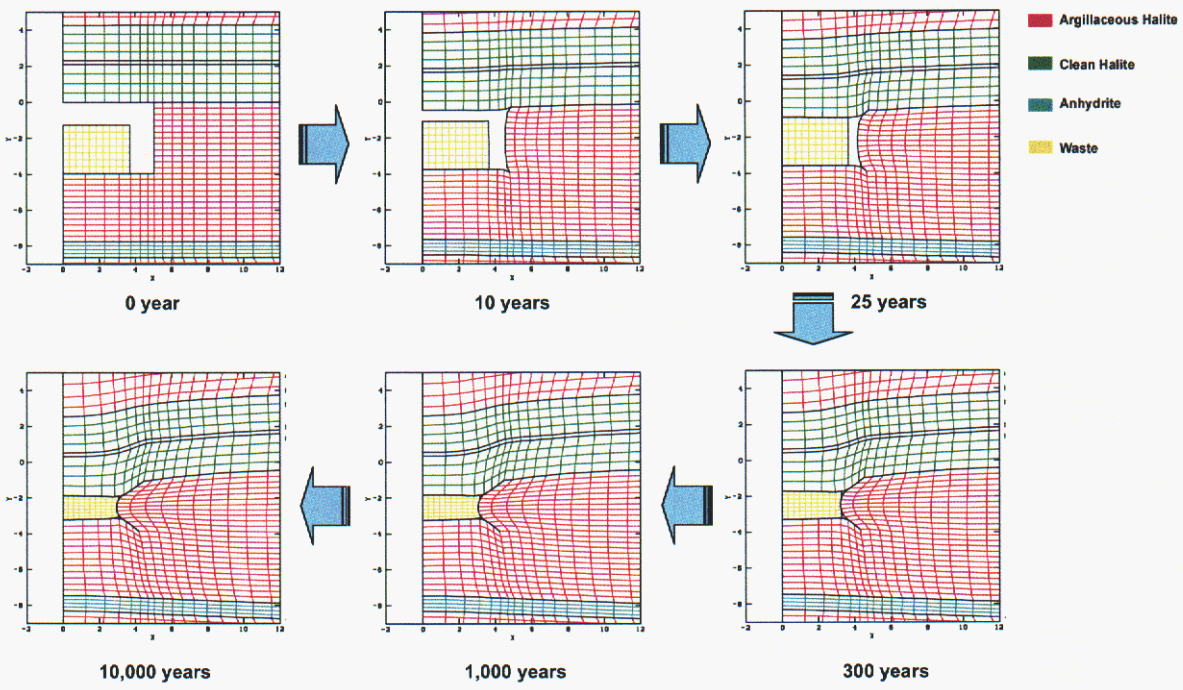

Figure 7: Deformation of Raised Disposal Room Containing Waste with Time for *f*=0.0.

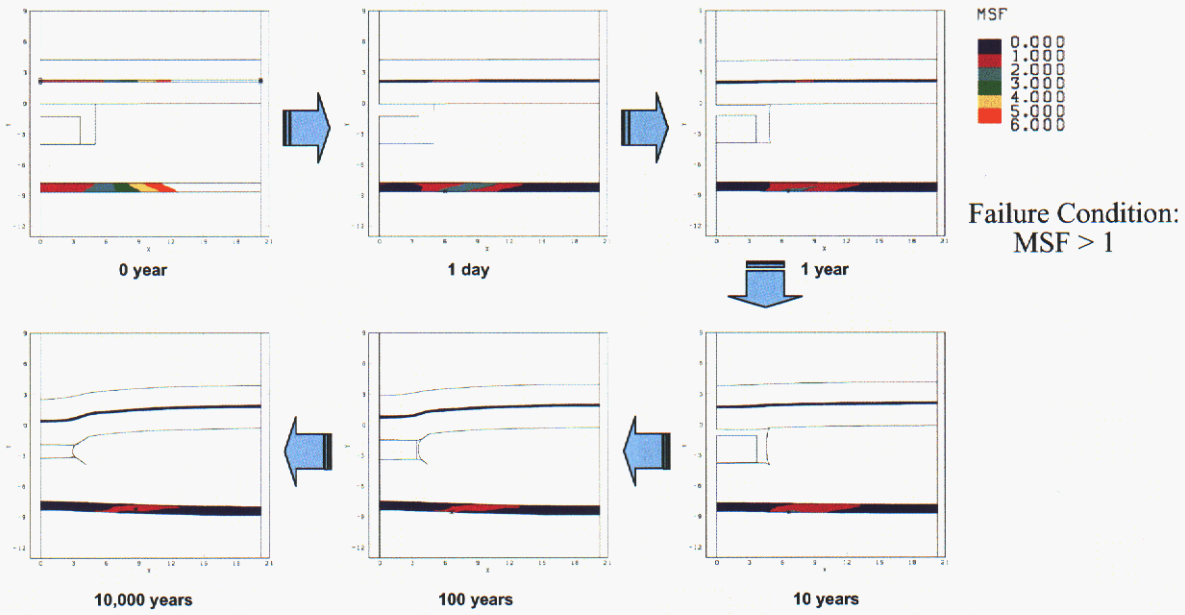

Figure 8: Anhydrite Shear Failure around the Raised Disposal Room with Time for *f*=0.0.

The above two figures show the dramatic deformation involved with the waste repository rooms. The primary mechanism of deformation is salt creep, which ensues with damage near the opening and without damage further out in the formation. Section 4 of this report will explore salt damage evaluation in greater detail. These snapshots of the DRZ over time represent some of the output of the Clay Seam G analyses. The DRZ model simply relates stress invariants and assumes that damage occurs based on the relation given in Figure 9. Thus the DRZ extends to its greatest dimensions relatively early in the repository regulatory period of 10,000 years. The report by Park and Holland (2003) contains several different situations for gas generation, and in all cases the DRZ vanishes early in repository history.

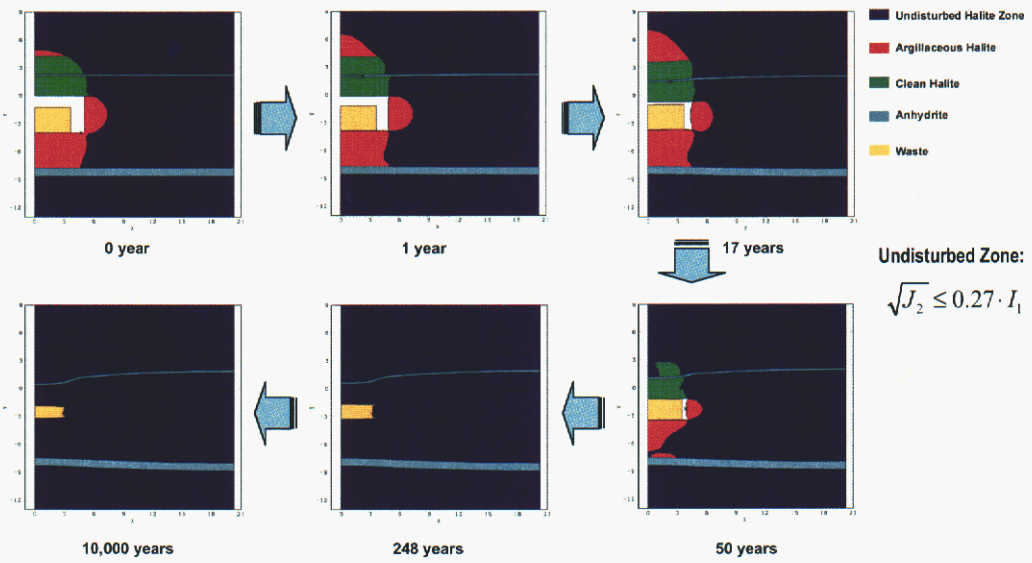

Figure 9: Disturbed Rock Zone around a Raised Disposal Room with Time for f=0.0.

3.3 Conclusions of Clay G Analyses

These calculations demonstrate that changing the repository horizon upward 2.43 meters has no appreciable effect on the response of the underground relative to the computations made for the CCA. This conclusion is drawn by first comparing new results with the previous results that underpinned the compliance application. The calculation procedures and input parameters were consistent with SAND97-0795 (Stone, 1997). These analyses used the same code, SANTOS, that supported the compliance calculations. A new validation and qualification of the software and hardware was assembled, as required by Quality Assurance procedures.

Performance Assessment. The hand-off to PA from the structural (finite element) calculations takes the form of a porosity surface. The models include geomechanical response of the Salado stratigraphy, the waste material, and gas generation in the disposal rooms. The volume change of the disposal room due to the salt creep is strongly dependent on the gas generation factor, *f*. The calculations used in the CCA were replicated and then repeated for grid changes appropriate for the new horizon to Clay Seam G. Because the CCA porosity surface calculated for the original horizon and the new porosity surface calculated for the raised rooms are essentially identical, no changes to the porosity surface are recommended to the compliance re-certification calculations.

Disturbed Rock Zone. Calculations of the DRZ illustrate several interesting features. First the propagation of the DRZ into the surrounding rock salt passes through Marker Bed 139 in the case of the original horizon (Park and Holland, 2003) and does not penetrate Marker Bed 139 in the case of the raised room, as shown above in Figure 9. Quantitatively, the extent of the DRZ can be summarized as follows:

- In the case of the raised room, the maximum thickness of DRZ is almost 6 meters above the room and 4 meters under the room.

- In the case of the original horizon, the maximum thickness of upper DRZ is about 6 meters, while the lower DRZ extends 5.6 meters through Marker Bed 139.

In all models the DRZ grows until the creeping salt impinges on the waste, at which time the stresses trend back toward equilibrium and the DRZ diminishes. In all the simulations, the DRZ disappears quickly relative to the regulatory period of 10,000 years.

Anhydrite Fracture. The anhydrite marker beds sustain states of stress that promote failure. In addition, deformation into the room by the marker beds is substantial. Therefore, fracture of the anhydrite in the proximity of the disposal rooms is most probable and the strain (deformation) induced during room closure would ensure some anhydrite fractures would exist in the proximity of the disposal room. The internal gas pressure of the room does not affect characteristics of the shear failure zone in the anhydrite layer. Deviatoric stress conditions become less severe over time, but the damaged anhydrite is not expected to heal in a manner expected of the salt DRZ.

Anhydrite marker beds reside in the proximity of the disposal rooms, whether the room is at the original horizon or at the elevated horizon. Therefore, fractured anhydrite, possessing high permeability, resides intimate to the deformed room. High fluid pressure that could develop in disposal rooms would be expected to communicate readily and flow preferentially out the damaged marker beds.

4.0 Salt Damage Evaluations

The first three sections of this report summarize the current understanding of the geomechanical setting at WIPP, and the implementation of that state of knowledge against changes made to the repository since the initial compliance determination. This section presents much of the technical bases that buttress the choices made to address the changes. The discussion begins with first principles of the creation, evolution and attendant properties of the DRZ. The theory is expanded into laboratory test results, small-scale *in situ* experiments and full-scale analogs from industry experiences and international collaborations. These technical arguments provide reasoning for the parameter distributions and grid refinements selected for re-certification calculations, which must address changes to the underground as well as incorporate any advancement benefiting the collective state of knowledge. The ensuing discussion concentrates on rock salt damage, modeling, and properties, and provides objective evidence that the theory extends into practice sufficiently that the proposed analyses of the operating repository are reasonable and justified.

4.1 Principles of Salt Damage

Similar to underground structures sited in other geologic media, excavation of an opening, such as a drift, disposal room or shaft at the WIPP alters the virgin state of stress (i.e., $\sigma_1 \approx \sigma_2 \approx \sigma_3$) that exists in the rock salt. The rock zone proximal to the opening experiences deviatoric (or shear) states of stress ($\sigma_1 > \sigma_2 > \sigma_3$) after excavation. Because of the stress-concentrating effect of the opening itself, the deviatoric stresses are highest in the rock salt near the opening, especially near abrupt changes in opening geometry (e.g., corners), and decrease rapidly with distance from the opening. In addition to opening geometry and spatial position, other factors affecting the magnitude of the induced deviatoric stress include local geology (e.g., homogeneous versus layered media) and depth of the opening below ground surface because, absent tectonic influences, the stress magnitude is approximately proportional to depth. Because salt is a creeping medium, the stress differences are maximized upon excavation, and decrease thereafter.

In salt, deviatoric states of stress activate three deformation processes: (1) elastic, (2) inelastic viscoplastic flow, and (3) inelastic damage-induced flow[1]. Elastic deformations occur instantaneously (time-independent) in response to changes in stress state, while the two inelastic mechanisms are time-dependent, which gives salt its well-known creep characteristics. Inelastic flow models usually include stress and temperature terms, but the flow rate also depends on factors such as stress history and relative humidity.

Viscoplastic flow of salt has been well characterized for WIPP applications. Much of the most pertinent literature derives from WIPP research and development (e.g., Munson, 1979; Carter and Hansen, 1983; Munson and Dawson, 1984) but the WIPP history of salt deformation benefits from international collaboration (e.g., Langer, 1984; Wallner, 1984; Aubertin et al., 1991; Cristescu and Hunsche, 1992, to name a few). Plastic deformation occurs by dislocation motion within the salt lattice. The various dislocation mechanisms of concern to repository sciences are also well documented and include dislocation multiplication, glide, cross slip, and climb. Because viscoplastic flow is an isochoric or incompressible process, it does not induce damage to the salt matrix. In salt, dislocation mechanisms are activated by virtually all deviatoric stress states regardless of the magnitude of the applied mean stress (average of the three principal stresses). The physics and the mathematics are well established for models that represent viscoplastic flow.

In contrast to viscoplastic flow, damage-induced flow in salt is less well understood. Damage only occurs when the deviatoric stresses are relatively high compared to the applied mean stress and is manifested through the time-dependent initiation, growth, and coalescence of microfractures. Modeling approaches have been suggested for the microfracturing process, with limited success. For example, predictions of damage space for WIPP applications seem to represent what is witnessed in the underground in a qualitative sense. Indeed, point-wise geophysical measurements often validate the general sense of the damage model. However, a model for spatial and temporal damage evolution that includes prediction of permeability is not yet available to salt repository sciences.

---

[1] Sometimes referred to as stress-induced damage.

In terms of WIPP repository applications, one of the most important features of salt as an isolation medium is its ability to heal previously damaged areas. Damage recovery is often referred to as healing in geomechanics parlance. Healing arises when the magnitude of the deviatoric stress decreases relative to the applied mean stress. A decrease in deviatoric stress occurs as stresses approach lithostatic conditions, as would be the circumstance adjacent to a rigid inclusion such as Option D panel closures. The healing mechanisms include microfracture closure and bonding of fracture surfaces. Microfracture closure is a mechanical response to increased compressive stress applied normal to the fractures, while bonding of fracture surfaces occurs either through crystal plasticity, a relatively slow process, or pressure solution and re-deposition, a relatively rapid process (Spiers et al., 1988). Evidence for healing has been obtained in laboratory experiments, small-scale tests at WIPP and through observations of natural analogs as described later. Healing the salt DRZ can readily restore damaged salt to a low permeability as discussed in Section 4.5.

The discussion of salt behavior and deformation processes around WIPP openings lead to the following general observations about the DRZ:

- Microfracturing of the salt initiates immediately upon excavation of the openings and continues with time.
- Microfracture density and growth rates are highest near the opening and decrease with distance away from the opening
- Fracture growth in the DRZ will be anisotropic with fractures aligning parallel to the most compressive stress (the most compressive stresses are typically aligned parallel to the free surfaces of the openings).
- Over time, macrofracturing will lead to salt failure including floor heave, roof falls and rib slabbing and spalling.
- Salt damage is reversible. Rigid panel closures placed in WIPP openings will create a nearly hydrostatic state of stress in the DRZ adjacent to the inclusion.

4.2 Hydrologic Properties of Damaged Salt

Most geologic media, including salt, contain natural porosity in the form of interconnected channels and isolated inclusions. Fluid flow through such media is necessarily constrained to the interconnected porosity. In pure WIPP salt, the natural porosity is on the order of 1 percent or less and not well connected. In argillaceous WIPP salt, the porosity is marginally higher and fluid flow has been observed, although at very low rates (Beauheim and Roberts, 2002). The porosity of WIPP salt is filled with brine containing dissolved gases, principally nitrogen. Because salt creeps, pore pressures in the brine-filled pores would be expected to approach lithostatic. At the depth of the repository, the lithostatic pressure has been established at 14.9 MPa.

The porosity of the salt in the DRZ is higher than in the surrounding virgin rock because of the dilation induced by microfracturing, as explained above. Peach (1991) studied the effects of salt dilation using percolation theory and found that small levels of dilation (as little as 0.05 percent)

were sufficient to develop an interconnected pore network that formed primarily along grain boundaries. Furthermore, permeability through this network was found to be proportional to $(\varepsilon_{dv})^3$, where (ε_{dv}) is the dilatant volumetric strain equivalent to $\Delta V/V$ with ΔV and V representing the change in volume due to dilation and the initial volume, respectively. Assuming a dilatant strain of 0.5 percent (a value that could easily occur in the DRZ), the 0.05 threshold strain, and the Peach proportionality, the permeability within the DRZ could increase by at least three orders of magnitude. As shown later, Pfeifle et al. (1998) conducted permeability tests on WIPP salt specimens that had been deformed in the laboratory to volumetric strains of the order of 0.5 percent and estimated permeabilities that ranged from 10^{-15} to 10^{-14} m^2, at least seven orders-of-magnitude higher than observed in the field by Beauheim and Roberts (2002) for virgin argillaceous salt emphasizing the extreme sensitivity of WIPP salt permeability to small dilatant volumetric strains.

Utility of this simple model is complicated by the anisotropy of damage in the field. As will be shown throughout this section, fractures in salt develop with preferential orientation with respect to the stress state. As clearly shown in Figures 2 and 5, fractures *in situ* are generally parallel to the drift and perpendicular to the minimum principal stress. Permeability along the fractures, parallel to the drift would be much higher than permeability perpendicular to the drift. The anisotropic nature of fractures and the sensitivity to damage (i.e., the permeability increases by orders of magnitude with relatively low levels of damage) are two features that complicate development of a damage/permeability relationship for field applications.

Because of the sensitivity between salt permeability and dilation, the DRZ is expected to exhibit high permeability immediately adjacent to the WIPP openings and decrease away from the opening in direct relation to the level of induced damage and deviatoric stresses. The microfracturing will also relieve the pore pressure in the DRZ. At the free surface of the opening, the pore pressure will be atmospheric, while at depth the pore pressure will be on the order of 14.9 MPa. This pressure gradient through the DRZ will release brine into the opening. The pore pressure in the salt some distance beyond the DRZ may be lower than 14.9 MPa because the alteration of the stress field resulting from the excavation may relieve some stress acting on the isolated brine-filled pores even though the change in stress is not sufficient to induce damage. Because healing processes reduce porosity, permeability is expected to decrease when hydrostatic states of stress activate healing processes, particularly in the vicinity of rigid panel closures.

4.3 Laboratory Studies of Salt Damage

Laboratory studies provide the most readily attainable setting for testing material properties. The materials of interest to the Option D panel closure system include intact salt, damaged salt, salt-based concrete and anhydrite. The geomechanical calculations being conducted in support of WIPP re-certification activities have added detail in the representation of salt damage (and healing) and salt-based concrete materials. Both elements are more representative of actual conditions than previously modeled in the CCA calculations. Laboratory characterization of salt damage and healing is summarized in the following section and discussion of salt-based concrete properties is found in Appendix A, Section 4.6 and Section 4.9.

Extensive research has been conducted in the laboratory to determine both the deformational and hydrological behavior of WIPP salt. Early work focused on the characterization of the elastic and inelastic viscoplastic flow properties of salt (e.g., Hansen and Mellegard, 1977; Wawersik and Hannum, 1979, Hansen and Mellegard, 1980; Senseny, 1986; Mellegard and Pfeifle, 1993). Most of the early studies provided parameters for the WIPP creep model. This model is popularly known as the Munson-Dawson (1984) Model, or M-D Model. In fact the author (Munson) called the model the M-D Model to denote multimechanism-deformation. The constant-volume creep behavior of the underground modeled by M-D was validated against large-scale thermomechanical experiments. This background information was available for the use in the PA and the compliance certification application.

The phenomena associated with salt fracture were made obvious from observations in the WIPP underground (Section 4.6) and geophysical measurements (Section 4.7). Despite an acknowledged importance of salt damage to the WIPP repository, the DRZ was given a rather rudimentary treatment in the compliance calculations. As preparations are being made for the re-certification of regulatory compliance, additional sophistication is brought to the treatment of the DRZ. A large amount of the data available to quantify DRZ properties derives from laboratory studies that were performed to parameterize the M-D model. Eventually, systematic studies of salt fracture were undertaken in the laboratory. Based on field observations, experiments, and theory, salt damage is reversible. Therefore, consideration of the salt DRZ includes its creation, growth, and properties, as well as the conditions under which the DRZ would heal. The properties of the DRZ provide the crux of the modeling issues for the Option D panel closures.

Van Sambeek et al. (1993a) re-examined the extensive creep data existing from years of experiments on salt. Their hypothesis was that damage could be assessed because volumetric strain and principal stresses are carefully controlled test parameters. Stress states that led to dilation were defined in terms of stress invariants rather than individual stress components because the stress components for one type of test could not be compared directly with the stress components of another type of test. The two stress invariants selected were the first invariant of the traditional Cauchy stress tensor, I_1, and the second invariant of the deviatoric stress tensor, J_2. These invariants are related to mean (or confining) stress and deviatoric stress, respectively, and are defined as follows:

$$I_1 = 3\sigma_m = \sigma_1 + \sigma_2 + \sigma_3$$

$$J_2^{1/2} = \left\{ \frac{1}{6} \left[(\sigma_1 - \sigma_2)^2 + (\sigma_2 - \sigma_3)^2 + (\sigma_3 - \sigma_1)^2 \right] \right\}^{1/2}$$

where σ_m is the mean stress and σ_1, σ_2, and σ_3 are the three principal stress components for a particular type of test. Using these definitions, Van Sambeek et al. (1993a) plotted the stress states (in terms of invariants) that both did and did not induce dilation in WIPP salt as shown in Figure 10. In addition, laboratory data for Avery Island, Louisiana, domal salt were plotted, as many experiments had been conducted on Avery Island salt over the years. As shown, a clear delineation in the $I_1 - J_2$ stress space exists between conditions that cause dilation and those that do not regardless of the type of salt or type of test considered. Van Sambeek et al. (1993a)

suggested an empirical relationship to divide dilating stress states from non-dilating stress states and expressed this empirical relationship as follows:

$$\sqrt{J_2} = 0.27 I_1$$

This relationship is often referred to as the stress-invariant model and is used to predict dilational states of stress for WIPP salt.

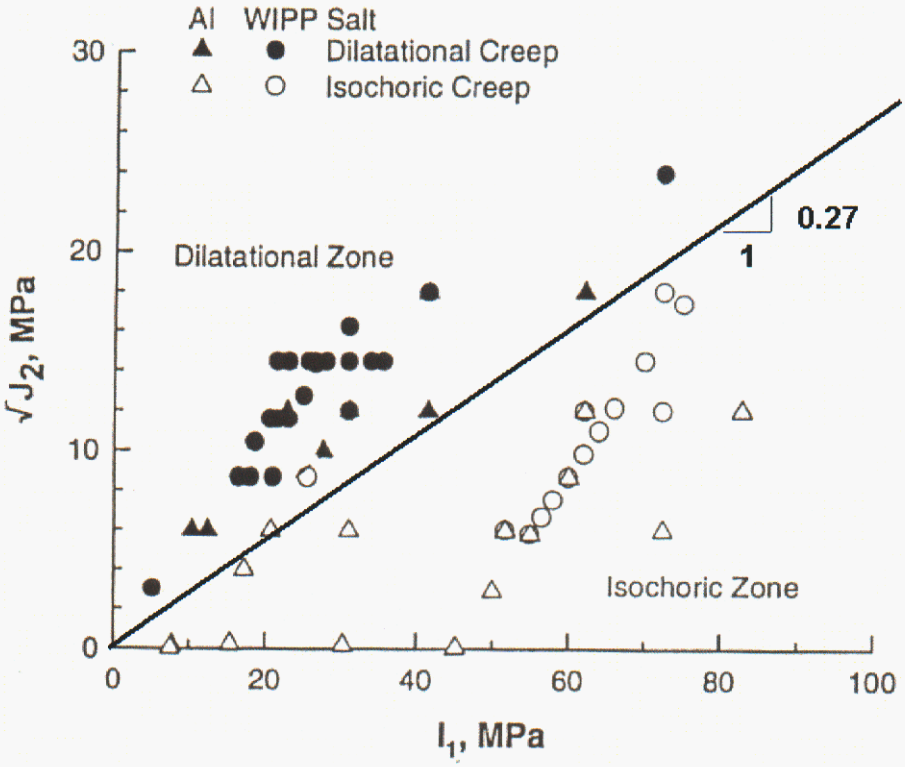

Figure 10. Stress States Known to Cause Dilation of WIPP Salt.

Stormont (1990) and Pfeifle et al. (1998) conducted laboratory tests on WIPP salt to correlate permeability with damage level expressed as dilatant volumetric strain. Figure 11 provides the results of these two studies and shows that permeability changes by nearly 10 orders-of-magnitude from less than 10^{-21} m^2 to more than 10^{-12} m^2 corresponding to changes in dilatant volumetric strain (or porosity) of up to 4 percent. These data are consistent with the range in permeability used in the PAVT.

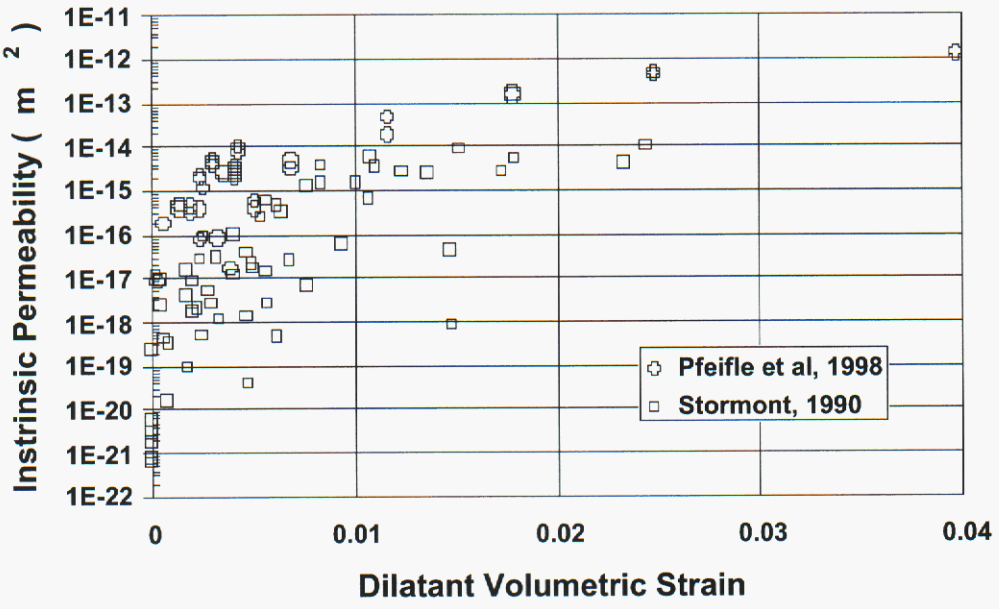

Figure 11. Permeability Versus Dilatant Volumetric Strain for WIPP Salt.

4.4 Salt Damage Modeling

The investigations of damage evolution are international issues. The WIPP science advisor (Sandia National Laboratories) has a long-standing collaboration with peers in European salt programs, most notably with the Bundesanstalt für Geowissenschaften und Rohstoffe (BGR). Salt researchers at the BGR have led development of a constitutive relationship between dilatancy and permeability (e.g., Hunsche and Schulze, 2000; Cristescu and Hunsche, 1998). Their experiments and theory show that dilatancy (also called volume change or damage) is linearly increasing with creep deformation under dilatant conditions and decreasing or healing with time in the compressive domain. This collaborative research is continuing. As noted by the Peer Review Panel (See Section 2.4) in their deliberations *constitutive models based on measurement of the influence of creep damage on hydrologic properties may be feasible in the future, but such models are not expected to indicate that the changed model has failed to conservatively bound repository performance* (Caporuscio et al., 2003).

The stress-invariant dilatancy model has been used in structural calculations for approximately 10 years and remains a viable tool for engineering purposes and can be coupled with numerical analyses to predict disturbed or damaged zones around a typical waste disposal room, as shown in Section 3.2. Figure 12 depicts the disturbed zone in terms of a damage factor, D, 40 years after excavation. In the region corresponding to $D > 1$, the stress states fall within the dilational zone, while in the region corresponding to $0.8 < D < 1.0$, the stress states remain in the isochoric zone (non-dilating zone) but are very near the dilational limit expressed by the stress-invariant model. As shown, the damaged zone or DRZ ($D > 1$) extends away from the room approximately 3 meters or more after 40 years of unobstructed closure.

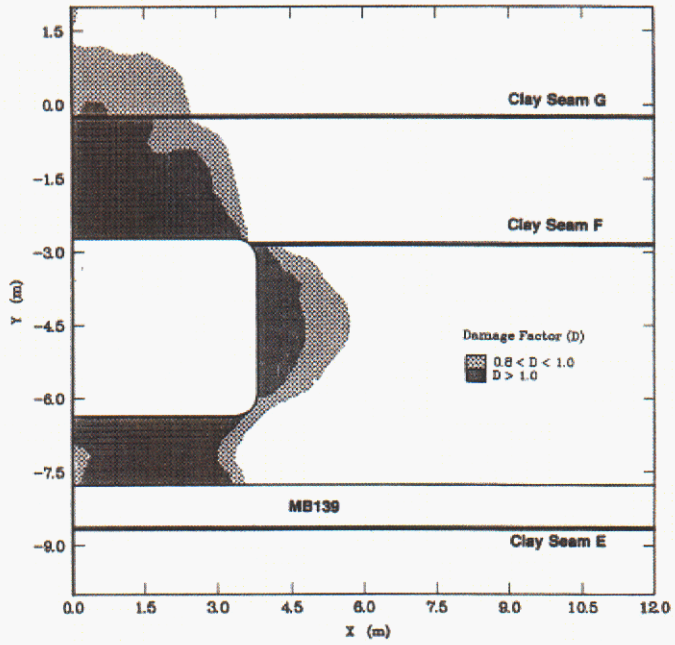

Figure 12. Damage Predicted Around a Typical WIPP Disposal Room 40 Years After Excavation (after Van Sambeek et al., 1993b).

The stress-invariant model described above can be used to predict the extent of the DRZ around openings in salt but quantifies neither the level of damage nor the increase in permeability associated with the DRZ. Based on the theoretical discussions provided above, the salt nearest an opening is expected to undergo the greatest damage and, as a corollary, will also experience the greatest increase in permeability. Salt farther from the opening undergoes much less damage and, as a result, experiences a much smaller change in permeability.

4.5 Salt Damage Healing in Laboratory Studies

In laboratory tests Costin and Wawersik (1980), Brodsky (1990) and Pfeifle and Hurtado (1998) have shown that the damage evolution process in salt is reversible through crack closure and healing. In the Costin and Wawersik study, a series of short-rod fracture toughness strength tests were performed to determine the tensile load required to initiate and propagate fractures in WIPP salt. The fractured test specimens were subsequently subjected to healing hydrostatic compressive stresses ranging from 10 to 35 MPa, and then retested in a second series of fracture toughness tests after healing times of varying length. The study showed that the healed specimens regained from 70 to 80 percent of their initial fracture toughness strength.

Using the well-known correlation between wave velocity and crack development in geologic materials, Brodsky (1990) used compressional ultrasonic wave measurements to study crack initiation, propagation and healing of WIPP salt. In general, velocity decreases with increases in

rock dilation and increases in response to crack closure and/or porosity reduction. Microcracks were introduced into WIPP salt specimens during constant strain-rate triaxial compression tests conducted at low confining pressure. After specified damage levels were induced, hydrostatic compressive stresses of 5, 10, or 15 MPa were applied to the damaged specimens to promote healing. During both the loading and healing stages of the tests, ultrasonic wave transducers were mounted directly on the test specimens to monitor wave velocity parallel and perpendicular to the maximum principal compressive stress. During loading, wave velocity parallel to the maximum principal stress decreased 1 to 2 percent, while velocity perpendicular to the maximum principal stress decreased by as much as 10 percent. In contrast, velocity measurements made during healing (or fracture closure) increased, with the rate of increase depending on the initial level of damage and the magnitude of the applied hydrostatic stress. The rate of increase in the wave speeds was slower for the more highly damaged specimens and this finding was attributed to shear offsets along the fractures. Rates of increase in velocity were ordered with respect to hydrostatic stress with higher rates corresponding to the higher hydrostatic stress levels applied during healing. Velocity recovery generally occurred within a few days.

Pfeifle and Hurtado (1998) studied salt healing through a series of gas and brine permeability tests conducted on damaged WIPP salt specimens subjected to compressive hydrostatic stresses of 1, 5, 10 and 15 MPa. Damage was initially introduced through constant stress creep tests conducted at low confining pressure. The damaged specimens were then loaded hydrostatically to promote healing and permeability measurements were made as a function of time. Permeability decreased as a function of time with larger decreases corresponding to higher hydrostatic stress levels and specimens saturated with brine rather than gas. In some tests, permeability decreased by nearly two orders-of-magnitude in less than 30 days. The permeability data were used to estimate healing time constants that could then be used to predict the time required for complete healing. Based on their results, complete healing requires several hundreds of years at very low hydrostatic stress states (1 to 5 MPa), but is of the order of only a few years for higher hydrostatic stress states (i.e., 10 and 15 MPa).

4.6 Salt Damage Healing—*In Situ* Small Scale

The laboratory data for salt damage characteristics, healing and salt-based concrete properties are all germane to the DRZ issues, particularly as applied for Option D panel closures. However, implementation of closures at WIPP involves much larger scales and uncertainties associated with up-scaling properties. This section presents additional information regarding the DRZ and seal material performance *in situ*.

A series of sealing experiments in the WIPP underground were executed over a ten-year period from 1985 to 1995. Series A and B are particularly relevant to panel closures, as they comprised vertical (A) and lateral (B) placement of salt-based concrete. Many technical publications on the Small Scale Seal Performance Test (SSSPT) program have been prepared and are summarized in Finley and Tillerson (1992). Series A and B utilized nine emplacement holes located in the floor of the D Room Alcove and in the west rib of Room M. The seal material was an expansive-salt concrete developed by Waterways Experiment Station (Wakeley and Walley, 1986).

All nine salt-based concrete seals performed well (Knowles and Howard, 1996). The larger (91-cm diameter) horizontal seals are most closely analogous to panel closures, and are described in more detail here. The concrete was pumped into forms and was not vibrated (Stormont and Howard, 1986). The seal system consists of the seal material, the seal/host rock interface, the zone of rock immediately surrounding the seal, and the far-field host rock. The seals were tested for gas and brine permeability from 1985 to 1987 and again from 1993 to 1995. The tests did not provide information regarding the flow paths of the test fluid, so the calculated system permeability represents a composite fluid barrier presented by all components of the seal system. Gas permeability determined in 1985-1987 ranged from 10^{-17} to 10^{-20} m^2 and improved to 10^{-19} to 10^{-23} m^2 when re-tested between 1993-1995. Additional geophysical and petrographic studies conducted in concert with the flow testing of the concrete seals (Knowles et al., 1998) provided evidence that the damage existed on both sides of the concrete plug. Therefore, the rigid concrete inclusion provided the requisite back stress to heal the extant DRZ.

4.7 DRZ Delineation by Sonic Velocity

A considerable body of geophysical investigative work has been completed in the WIPP underground in the period since the initial certification (Holcomb, 1999, Hardy and Holcomb, 2000, Holcomb and Hardy, 2001). In most investigations, Holcomb and co-workers delineated the WIPP DRZ as a function of depth orthogonal to a drift wall and along vertical and horizontal paths parallel to the wall. In one campaign, they measured velocity in holes oriented at angle to the walls. The borehole array and the transducer assemblies allow measurement of elastic wave velocities necessary to detect the anisotropy of cracking associated with the DRZ. Velocity and attenuation of elastic waves in the salt are a function of the density of cracks, as is the permeability.

Cross-hole and same-hole velocity measurements give a consistent picture of the DRZ around the Q room access drift. The DRZ is well developed at mid-height on the rib, extending into the rock 2 meters and possibly as much as 4 meters. Near the back and floor, the DRZ is shallow (1 meter or less) or not detectable. Compressional mode (P) waves in same-hole measurements are most sensitive to the DRZ because of favorable orientation of particle motion perpendicular to the cracking. Changes in V_P as large as 22 percent were observed for P waves propagating perpendicular to the drift axis at room mid-height.

Open cracks and loosened grain boundaries decrease elastic moduli and therefore, elastic wave velocities. The effect on elastic wave velocities is strongest for cracks oriented perpendicular to the particle motion induced by the wave. Thus the physical extent of the disturbed zone can be determined by propagating elastic waves through successive portions of the formation until an undisturbed zone is reached, as indicated by a constant velocity with increasing depth from the rib. Cracking responsible for the disturbed zone is expected to vary as a function of distance from the walls of the Room Q alcove and to depend on the position of the measurement path relative to the back, floor and corner.

Cross-hole measurement paths were nominally one meter long, while the same-hole measurements all had the same fixed path length of 33 cm. Figure 13 shows the arrangement

and naming scheme for the measurement holes, QGU30, QGU31, … QGU41. Travel time measurements were made using the technique commonly used for laboratory determinations of sound speed in rock; a sound pulse was applied to the rock at a known time and place and, after traveling through the rock, was received by a transducer at a known distance. The travel time and distance combine to give the average velocity over that path.

The most recent work completed at WIPP probed twelve holes cored in the Room Q alcove corner (see Figure 13). Two rows of holes, 1 and 3 counting from the top, were in halite, while rows 2 and 4 were in argillaceous salt. Each hole was 10.16 cm (4 inches) in diameter, 6+ meters deep and as nearly horizontal as possible. Hole locations were chosen to sample the map units present (labeled halite and argillaceous in Figure 13), and also the expected variation in damage around the corner.

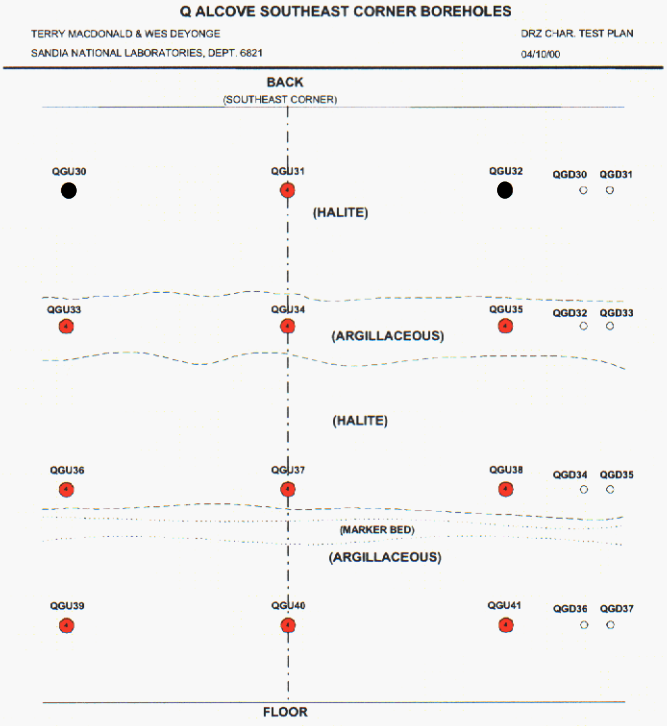

Figure 13. Layout of Holes for Room Q Alcove, with holes used for ultrasound measurements indicated in red. Other holes indicated are for proposed hydrological studies.

Sonic velocities can be measured vertically and horizontally across holes, resulting in 9 sets of measurements for vertical paths and 8 horizontal paths in planes parallel to the corner walls. In addition, twelve same-hole measurement sets were completed. Typical same-hole, P-wave results are shown in Figure 14. The DRZ of less than 2 meters developed along the wall (red dots) is typical for WIPP openings. The unique aspect of these measurements is the lack of DRZ

in the zone directly outside the room corner. As seen in Section 4.8, the damage fracture orientations also reflect stress states along the walls toward the corner.

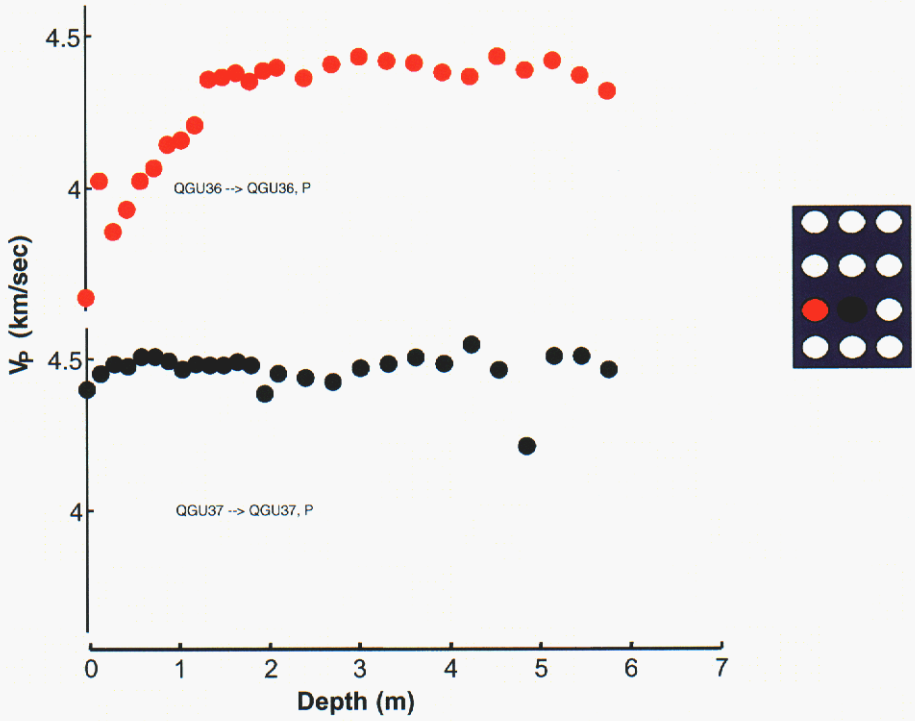

Figure 14. Same-hole measurements for adjacent holes, one in the left-hand wall (red) and in the corner (black).

Results show that velocity at depths greater than about 1 meter vary from the mean by less than 0.5%, which is close to the attainable accuracy. Similarly constant velocities are observed in the other paths through halite. In contrast, V_P along paths in the "argillaceous" halite layers varies by several percent even at depths beyond the DRZ. All four data sets for the horizontal cross-hole V_P measurements made in halite layers indicate a constant velocity as the measurement depth approaches 6 meters. Two data sets show clear evidence of a disturbed zone extending in about one meter. Little or no evidence for a DRZ was found in the other two measurements in halite. In contrast to horizontal paths, damage measured along vertical paths is less extensive, reaching shallower depths and producing smaller changes in V_P. The general pattern of damage is similar and slightly asymmetric, with greatest damage observed in the upper portion of the left wall and the lower portion of the right wall.

Previous work (Holcomb and Hardy, 2001) in the access drift leading into the Q room alcove, showed a simpler pattern of DRZ development and a more extensive damaged zone. In the access drift, where the geometry is essentially 2-dimensional, the DRZ was observed to be best developed at mid-height of the drift and to extend as much as two meters. The complexity

observed in the corners reflects the influence of the 3-dimensional geometry on the stress state and subsequent development of the DRZ.

Damage along the measurement path contributes to velocity decrease, which is a signature of the DRZ. Thus the constant V_P observed in the alcove corner along vertical paths indicates that no point from ceiling to floor has experienced significant damage in the form of cracks that could decrease the speed of a compressional wave propagating vertically. Cracks oriented perpendicular to the direction of propagation are most effective in decreasing V_P ; in this case, horizontal cracks would be most effective. Thus it appears that little or no horizontal cracking has occurred near the bisecting plane of the corner, at any depth, even 12 years after excavation. A meter away, the stress state is sufficiently different that V_P in the vertical direction is decreased, indicating some horizontal, or at least non-vertical, cracking did occur. Near the floor and ceiling the DRZ was less pronounced than in similar zones closer to the mid-height of the room. Damage was clearly anisotropic, with the maximum decrease in V_P being observed in directions more nearly perpendicular to the walls. This fits with the assumption that the DRZ is the result of cracks opening in the direction of minimum compressive stress. In previous work, velocity measurements typically indicate a DRZ extending in about 2 meters. An exception to that rule was found in the AIS (Hardy and Holcomb, 2000) where the DRZ only extends 0.5 to 1 meters. In the corner of the Room Q alcove the DRZ only extended in about 1 meter and there were many areas that did not appear to be damaged.

It is expected that the current results will be useful to other studies of the long-term deformation characteristics of salt. The data delineate the DRZ as a function of depth from the alcove corner and as a function of the varying stress state around a rectangular alcove corner cross-section. The significance of the results lies in the length of time the DRZ has had to develop (approximately 12 years), the geometrical complexity of the alcove corner, which will allow a more rigorous test of models than is possible in simpler geometries. Understanding the time-dependent changes in damage, and thus permeability, as the DRZ develops is important because these properties affect sealing and PA models of underground openings at the WIPP.

Previous work had examined the DRZ in simple geometries, typically a room wall or a long drift. More recent work is an extensive look at what happens in the corner of a room, an area deliberately chosen for its complexity. As expected, the pattern of damage was found to be more complex than in the simpler geometries previously studied. Two features were unexpected: damage did not extend in nearly as far as in the previous studies, and along the bisecting axis of the corner, no DRZ at all was observed.

4.8 Observational Fracture Studies

The WIPP site itself provides an underground research setting that has been exploited to quantify spatial and temporal characteristics of the disturbed rock zone. In concert with the work of Holcomb and coworkers as summarized in the previous section, we have continued petrofabric analyses of salt core recovered from the sonic velocity holes. To complement these studies, international partners provided cores from the Asse Mine of interest to their programs. Together, these cores avail an opportunity to assess the nature of damaged core from the proximity of

underground openings in salt workings. In this section we present petrophysical evidence of the structural state of the DRZ and excavation disturbed zone cores drilled from two different sites.

The comprehensive microstructural examinations that include fracture, free dislocation density and subgrain boundaries have been submitted to the European Union for publication with their sponsored research on salt repositories. However, the relevant observations concern the manifestation of damage, which is described and quantified in terms of fractures. In addition to salt cores from WIPP, samples were provided by German colleagues from the ALOHA II Project (Wieczorek and Zimmer, 1999), and from the Northern Test Drift B of the German Thermal and Structural Demonstration Experiment (TSDE) Test Field. The TSDE was conducted at the Asse Mine, near Braunschweig, Germany, by Gesellschaft fur Anlagen- und Reaktorsicherheit mbH (GRS). BAMBUS II (Backfill and Material Behavior in Underground Salt repositories) is the post-facto evaluation of the TSDE, and addresses the behavior of the DRZ, as well as backfill material within a geologic repository for heat-generating radioactive waste in rock salt. Fracture analyses entail petrographic fracture mapping; creation of thick sections to investigate fracture densities, fracture apertures, fracture angles and the spatial distribution of fractures. For the most part scanning electron microscopy (SEM) was used to capture and quantify the images.

A larger suite of observational studies (Chapin and Hansen, 2002) focused on microstructural analyses of seven salt cores: (1) WIPP Core QGU14 (6.07 m), (2) WIPP Core QGU36 (7.33 m), (3) WIPP Core QGU39 (2.25 m), (4) Asse Mine Core DJ-V (6.97 m), (5) Asse Mine Core HD-V (6.83 m), (6) TSDE Core VVS-A-Mi4 (0.72 m), and (7) TSDE Core VVS-D1-Mi4 (0.77 m). The dimensions in parentheses indicate the lengths of the cores referenced from the opening or drift face in which the cores were recovered. As can be seen, most cores extend from a free surface to a considerable depth into the country rock. The TSDE cores were selected from the near field of the heater experiment. These cores exhibited little fracturing, despite being adjacent to a free surface. The associated elevated temperature gave rise to thermally activated deformational processes, thereby minimizing the brittle manifestations of fracture.

The geology of WIPP QGU14 and QGU36 are similar; both comprise elongate, coarse, clear halite and minor amounts of anhydrite. WIPP QGU39 derives from the so-called "argillaceous" salt zone. All WIPP core was obtained by dry drilling (horizontally) through the inside rib of the 4-m high repository drift. WIPP Core QGU14 was drilled normal to the rib at mid-height, whereas cores QGU36 and QGU39 were recovered from boreholes drilled into the corner of the Q-Room access drift at an angle of 45°–50° to the inside rib faces. The German cores derive from lined and unlined portions of 80-year-old drifts in the Asse research mine, at a depth of 700 meters (see Section 4.10). The TSDE cores were extracted from the Asse Mine's Northern Drift B, at the 800-m level as part of ongoing international collaborations.

Of the seven cores studied, three cores were analyzed over their entire length at a shallow distance into the rib: (1) WIPP Core QGU39 (2.25 m), (2) TSDE Core VVS-A-Mi4 (0.72 m), and (3) TSDE Core VVS-D1-Mi4 (0.77 m). The four remaining cores, WIPP Cores QGU14 (6.07 m) and QGU36 (7.33 m), as well as the ALOHA II Cores DJ-V (6.97 m) and HD-V (6.83 m) were analyzed differently. The complete first meter of each core was examined, and then subsequent fracture analyses were performed at 1-m intervals until the core length was exhausted. For display purposes Figure 15 plots the fracture distribution for the WIPP cores alone. Of the 744 fractures measured in the three WIPP cores, only two fractures at a depth of greater than 2 meters have measured apertures wider than 125 μm. In all the cores measured, fracture apertures are predominantly wider proximal to the rib face (at approximately 0.1 meters and 1.25 m). Cores QGU36 and QGU39 were oriented nearly 45° to the drift face. The measured fracture angles qualitatively oriented parallel to the drift wall, and thus could be categorized as stress induced fractures and clearly not coring damage. Fracture angles closest to the rib face lie subparallel to the rib face for both cores; at approximately 60° to the core axis in QGU36 and approximately 50° in core QGU39. At approximately 2 m, the fracture angles in both cores have rotated essentially normal to the core axis. Results of the fracture analyses of the WIPP, ALOHA II and TSDE salt cores are presented in Figure 16.

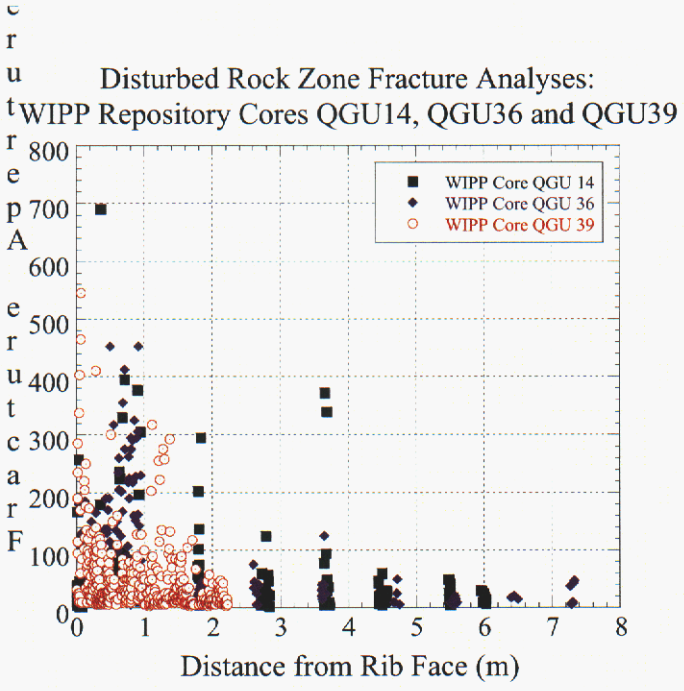

Figure 15. Fractures and Apertures in Three WIPP Cores.

A rather surprising result is that the fracture distributions and fracture apertures between ALOHA II Cores DJ-V and HD-V were found to be similar. One would hypothesize that the core obtained from behind the rigid tunnel lining (details given in Section 4.9) would have completely healed the fractures. Permeability measurements showed that permeability was

reduced behind the liner, despite the presence of fractures measured in the cores. Except for a few wide fractures measured proximal to the rib wall in core DJ-V, there does not appear to be a large disparity between fracture density and fracture aperture as a function of depth between either the ALOHA II lined (DJ-V) and unlined (HD-V) drift samples. Fracture distributions and fracture apertures are similar for both TSDE cores and minimal compared to the unheated cores. A comparison of all seven cores is presented in Figure 16. The highest density of fractures is observed closest to the rib walls, at an approximate distance ≤ 2 meters. Fracture apertures at a depth of 2 meters or greater are predominantly ≤ 100 µm wide.

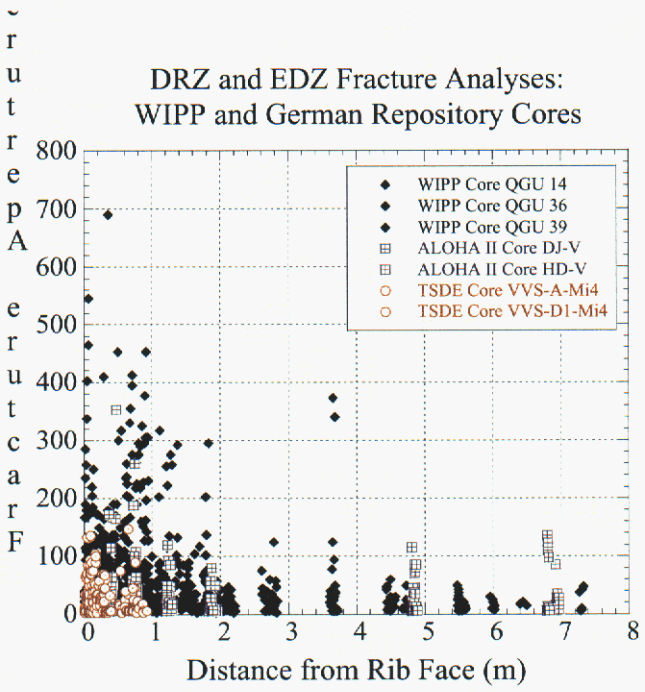

Figure 16. Fracture Apertures for DRZ Cores from WIPP and Asse

The microstructural analyses performed on cores reveals that the distribution of fractures is higher and that fracture apertures are wider proximal (approximately ≤ 2 meters) to the rib faces. Fracture apertures existing at a depth of 2 meters or greater are predominantly ≤ 100 µm wide. A clear, though qualitative relationship defining the DRZ exists between velocity and damage. Sonic velocity increases as damage decreases and the shapes of the curves are inversely proportional. It would appear that the DRZ exists as deep as 2 meters in the clean zones of salt near the rib midheight, and to a relatively lesser extent near the floor, near the back and near the corners.

4.9 Full-Scale Field Analogs

Salt damage healing has been demonstrated in the laboratory and in 1-m-scale field tests on WIPP salt. Field evidence of damage healing on a large scale has not been demonstrated within

the confines of WIPP. Indeed, in the world this type of information is sparse. The Germans have published an excellent example of healing around a rigid enclosure. This case study is known as ALOHA (Untersuchungen zur Auflockerungeszone um Hohlräume im Steinzalzgebirge). These investigations were conducted in the Asse salt mine near Braunschweig, Germany (Wieczorek and Zimmer, 1999).

The *in situ* permeability tests were conducted on the 700-m level of the Asse salt mine, where a cast steel bulkhead was placed in a drift during the 1920's. Tests were conducted in open sections of the drift and behind the steel liner. Permeability magnitudes are diagramed in Figure 17. As can be readily ascertained, the permeability tests evidence healing of the DRZ around a rigid structure, at a depth comparable to WIPP. The extension and the hydraulic properties of the DRZ around a drift were investigated by means of gas and liquid injection testing.

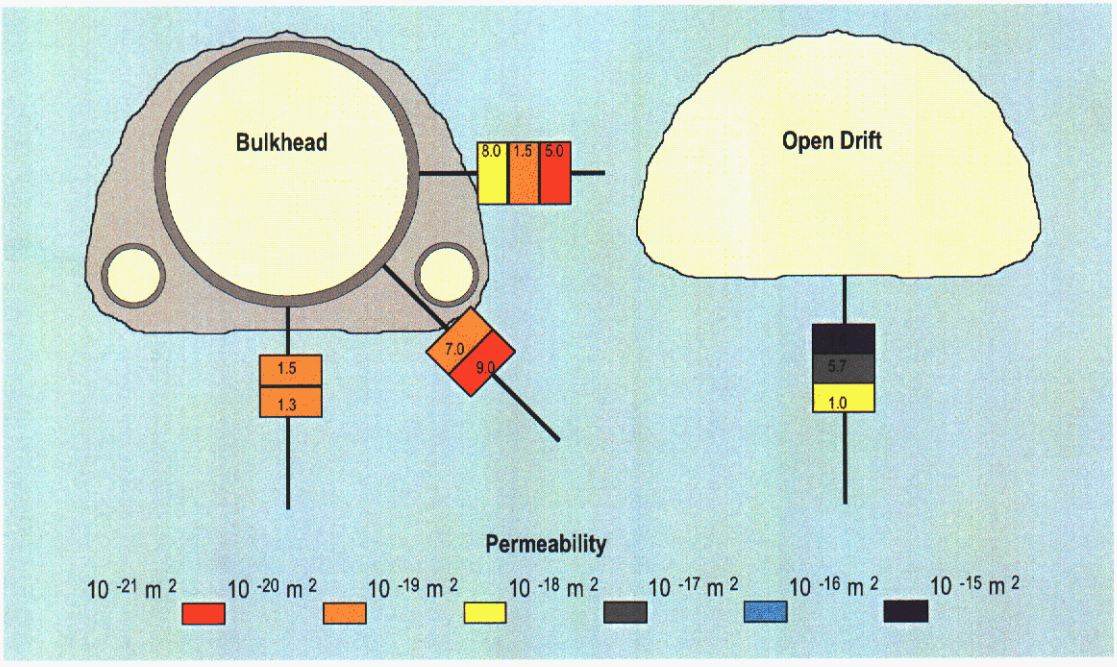

Figure 17. ALOHA2: Permeability Distribution around the Bulkhead and Open Drift.

Concrete bulkheads placed in Canadian potash mines also provide important case studies for both construction and performance. The most pertinent experience noted during a reconnaissance in 1994 occurred in the PCS Rocanville potash mine. Additional analog observations regarding Canadian bulkheads and other case studies are reported in Eyerman et al., 1995. The experience at the Rocanville mine is particularly illuminating because concrete seal construction was performed quickly, and success was critical to survival of the mine itself. This successful deployment of a drift seal constructed of brine-based concrete is analogous to panel closure construction at the WIPP.

The Rocanville bulkhead was constructed in halite, following water inflow from an overlying aquifer. A concrete bulkhead was designed to contain the inflow and prevent additional inflow into the mine. A "temporary" bulkhead located 120 ft from the face (point of inflow) was constructed, and has functioned perfectly since its emplacement in 1985. Total hydrostatic head is monitored by various accesses through the bulkhead. Design and construction of the bulkhead took only a few weeks, and the conditions for the construction were less than ideal. Despite these factors, the bulkhead has resisted water pressures approaching 10 MPa and has not leaked since construction. This does not demonstrate that the DRZ developed and then healed, but does demonstrate a full-scale salt-based concrete bulkhead in salt that is impermeable to a full hydrostatic head.

The principal reason this case study is so important to the future panel closure at WIPP is its simplicity and its overwhelming success. These factors demonstrate that basic salt concrete is highly impermeable and construction methods need not be overly elaborate to be successful.

The most relevant analogs to the case at hand include similar scale, setting, time and materials as the WIPP Option D Panel Closure. Time represents one element beyond the reach of laboratory or field tests. The fact that salt mines creep closed is well known. Ancient sections of the Hallstatt salt mine have preserved holdings dating from the Late Iron Age (500 B.C. to 0), including an unfortunate Celtic miner encapsulated in salt, whose "fully preserved body…was found in the Hallstatt salt mine" (DHP-Design, 2003). The fact that salt cavities creep closed is well recognized. Two pertinent analogs presented here illustrate that on a large scale, rigid inclusions tend to heal damaged salt and when functioning in tandem with salt provide essentially impermeable barriers.

5.0 Summary

This document presents the treatment of operational changes at the WIPP that include the disturbed rock zone among technical considerations. The flow of the document is chronological from the compliance certification, through the performance assessment verification, to the technical migration of the baseline in preparation for the re-certification calculations. Information within this report provides justification and reasonableness for the DRZ model in Salado flow calculations, parameters, and level of detail that will represent major changes experienced in the WIPP underground, namely, incorporation into performance assessment calculations 1) the EPA mandated Option D panel closure and 2) the advent of raising the repository horizon 2.43 meters to Clay G. Incorporation of these changes, which have occurred since the original compliance certification five years ago, required additional detail be added to the analysis scheme and that improvement to our understanding of the DRZ be included to reflect more accurately the actual conditions experienced in the WIPP nuclear waste repository.

These changes, particularly the Option D condition of the certification, represented significant departure from the analyses run for the original compliance PA and the verification test that followed the CCA. At the same time, the DRZ model was updated to depict more accurate geometries and properties of the DRZ. The operational reality of mining to Clay G was evaluated in terms of room closure and the resulting porosity, which in turn is sampled in PA.

Details of the Clay G analyses also provided insight to the local behavior of the DRZ evolution and devolution and the distortion of the anhydrite layers near the disposal rooms. This information supports the analytical treatment of the Option D panel closure and its incorporation into the Salado flow conceptual model. The updated modeling approaches and the concepts for the DRZ were subjected to independent peer review in accord with regulatory procedures and found to be acceptable.

The rest of this document provides a summary of technical information pertaining to the DRZ and emphasizes knowledge pertaining to WIPP that might change the methods implemented in previous analyses. Calculations show that prediction of the one-way evolution of the DRZ replicates observations in the WIPP underground. The size and shape of the DRZ around an opening based on a stress invariant criterion are similar to the size and shape derived from sonic velocity studies and from microscopy of core damage. The model output does not provide permeability directly, but the trend and magnitude of permeability around WIPP openings are understood in considerable detail. For WIPP applications, the high permeability in zones near the skin of a room is of little consequence. On the other hand, over estimation of the extent of the DRZ could impart significant fictitious effects, if modeled improperly. Healing of the DRZ—entombment of the waste—is a far more important concept to PA. Eventually DRZ evolution will reverse as the creeping salt approaches equilibrium with the disposal room contents—a condition that could arise quickly if a rigid panel closure were constructed. Salt healing will ensue and the technical bases, from theory to practice, for this fact are given in the main text.

A review of the compliance supporting documents and the compliance submittal itself was performed to assess various official positions on the DRZ as a matter of "record". Places within the record that mention the DRZ are listed in Appendix B. Contents of this document and its references include all the significant advancements pertaining to the DRZ and sufficient technical justification for model and parameter changes proposed for WIPP re-certification.

6.0 References

Aubertin, M., D.E. Gill, and B. Ladanyi. 1991. "Unified Viscoplastic Model for the Inelastic Flow of Alkali Halides," *Mechanics of Materials*. Vol. 11, no. 1, 63-82.

Beauheim, R.L., and R.M. Roberts. 2002. "Hydrology and Hydraulic Properties of a Bedded Evaporite Formation," *Journal of Hydrology*. Vol. 259, no. 1-4, 66-88.

Brodsky, N.S. 1990. *Crack Closure and Healing Studies in WIPP Salt Using Compressional Wave Velocity and Attenuation Measurements: Test Methods and Results*. SAND90-7076. Albuquerque, NM: Sandia National Laboratories.

Brodsky, N.S. 1995. *Thermomechanical Damage Recovery Parameters for Rock Salt from the Waste Isolation Pilot Plant.* SAND93-7111. Albuquerque, NM: Sandia National Laboratories.

Bryan, C.R., F.D. Hansen, D.M. Chapin, and A.C. Snider. 2001. "Characteristics of the Disturbed Rock Zone in Salt at the Waste Isolation Pilot Plant," *Rock Mechanics in the National Interest: Proceedings of the 38th U.S. Rock Mechanics Symposium, DC Rocks 2001, Washington, D.C., USA, 7-10 July, 2001.;* Eds. D. Elsworth, J.P. Tinucci, and K.A. Heasley. Exton, PA: A.A. Balkema. Vol. 1, 511-516.

Caporuscio, F., J. Gibbons, C. Li, and E. Oswald. 2003. "Salado Flow Conceptual Models Final Peer Review Report." Carlsbad, NM: U.S. Department of Energy, Carlsbad Field Office (Copy on file in the Sandia WIPP Records Center as ERMS# 526879).

Carter, N.L., and F.D. Hansen. 1983. "Creep of Rocksalt," *Tectonophysics*. Vol. 92, no. 4, 275-333.

Chapin, D.M., and F.D. Hansen. 2002. "Fracture Analyses (January 31, 2002 – July 31, 2002)." "Sandia National Laboratories Technical Baseline Reports, WBS 1.3.5.3." "Compliance Monitoring, WBS 1.3.5.4." "Repository Investigations, Milestone RI 03-210, July 31, 2002." Carlsbad, NM: Sandia National Laboratories. 5.1-1 to 5.1-9. (Copy on file in the Sandia WIPP Records Center as ERMS# 526049).

Costin, L.S., and W.R. Wawersik. 1980. *Crack Healing of Fractures in Rock Salt.* SAND80-0392. Albuquerque, NM: Sandia National Laboratories.

Cristescu, N. 1993. "A General Constitutive Equation for Transient and Stationary Creep of Rock Salt," *International Journal of Rock Mechanics and Mining Sciences & Geomechanics Abstracts*. Vol. 30, no. 2, 125-140.

Cristescu, N., and U. Hunsche. 1992. "Determination of a Nonassociated Constitutive Equation for Rock Salt from Experiments," *Finite Inelastic Deformations – Theory and Applications, IUTAM Symposium, Hannover, Germany, August 1991.* Eds. D. Besdo and E. Stein. New York, NY: Springer-Verlag. 511-523.

Cristescu, N., and U. Hunsche. 1998. *Time Effects in Rock Mechanics*. Series: Materials, Modeling and Computation. New York, NY: Wiley.

Dale, T.F., and L.D. Hurtado. 1998. "WIPP Air-Intake Shaft Disturbed Rock Zone Study," *The Mechanical Behavior of Salt, Proceedings of the Fourth Conference, Ecole Polytechnique, Montreal, Quebec, Canada, June 17 and 18, 1996.* Eds. M. Aubertin and H.R. Hardy, Jr. Clausthal-Zellerfeld, Germany: Trans Tech Publications. 525-535.

DHP-Design. 2003. "Short History of Hallstatt." Hallstatt-Online. http://222.hallstatt.net/besucher/geschichte/kurzfassung.php3?lang-en (accessed October 2003).

Eyermann, T.J., L.L. Van Sambeek, and F.D. Hansen. 1995. *Case Studies of Sealing Methods and Materials Used in the Salt and Potash Mining Industries*. SAND95-1120. Albuquerque, NM: Sandia National Laboratories.

Finley, R.E., and J.R. Tillerson. 1992. *WIPP Small Scale Seal Performance Tests - Status and Impacts*. SAND91-2247. Albuquerque, NM: Sandia National Laboratories.

Hansen, C.W. 2002. "Estimate of Change in Repository Releases Due to Changes in BRAGFLO Modeling." Memorandum to Kathryn Knowles, Sandia National Laboratories, Carlsbad, NM, 9 May 2002. Carlsbad, NM: Sandia National Laboratories (Copy on file in the Sandia WIPP Records Center as ERMS# 522233).

Hansen, C.W., and C.D. Leigh. 2002. "Sandia National Laboratories Carlsbad Programs Group Waste Isolation Pilot Plant, A Reconciliation of the CCA and PAVT Parameter Baselines, Revision 2." Carlsbad, NM: Sandia National Laboratories (Copy on file in the Sandia WIPP Records Center as ERMS# 524694).

Hansen, C.W., C.L. Leigh, and J.S. Stein. 2002. "Analysis Plan for the Impact Assessment of Alternate Panel Closure Systems." Analysis Plan AP-087, Revision 0. Carlsbad, NM: Sandia National Laboratories (Copy on file in the Sandia WIPP Records Center as ERMS# 522493)..

Hansen, F.D., and K.D. Mellegard. 1977. *Creep Behavior of Bedded Salt from Southeastern New Mexico at Elevated Temperature*. SAND79-7030. Albuquerque, NM: Sandia National Laboratories.

Hansen, F.D., and K.D. Mellegard. 1980. *Further Creep Behavior of Bedded Salt from Southeastern New Mexico at Elevated Temperature*. SAND80-7114. Albuquerque, NM: Sandia National Laboratories.

Hardy, R.D., and D.J. Holcomb. 2000. "Assessing the Disturbed Rock Zone (DRZ) Around a 655 Meter Vertical Shaft in Salt Using Ultrasonic Waves, an Update," *Pacific Rocks 2000, Proceedings of the Fourth North American Rock Mechanics Symposium, NARMS 2000, Seattle, Washington, USA, 30 July-3 August, 2000*. Eds. J. Girard, M. Liebman, C. Breeds, and T. Doe. Brookfield, VT: A.A. Balkema. 1353-1360.

Holcomb, D.J. 1999. "Assessing the Disturbed Rock Zone (DRZ) Around a 655 Meter Vertical Shaft in Salt Using Ultrasonic Waves," *Rock Mechanics for Industry: Proceedings of the 37th U.S. Rock Mechanics Symposium, Vail Rocks 99, Vail, Colorado, 6-9 June, 1999*. Eds. B. Amadei, R.L. Kranz, G.A. Scott, and P.H. Smeallie. Brookfield, VT: A.A. Balkema. Vol. 2, 965-972.

Holcomb, D.J., and R. D. Hardy. 2001. "Assessing the Disturbed Rock Zone (DRZ) at the Waste Isolation Pilot Plant in Salt Using Ultrasonic Waves," *Rock Mechanics in the National Interest, Proceedings of the 38th U.S. Rock Mechanics Symposium, DC Rocks, Washington, D.C., USA, 7-10 July, 2001*. Eds. D. Elsworth, J.P. Tinucci, and K.A. Heasley. Exton, PA: A.A. Balkema. Vol. 1, 489-496.

Howarth, S.M. and T. Christian-Frear. 1996. *Porosity, Single Phase Permeability, and Capillary Pressure Data from Preliminary Laboratory Experiments on Selected Samples From Marker Bed 139 at the Waste Isolation Pilot Plant. DRAFT.* SAND94-0472. Carlsbad, NM: Sandia National Laboratories (Copy on file in the Sandia WIPP Records Center as WPO# 38367).

Hunsche, U., and O. Schulze. 2000. "Measurement and Calculation of the Evolution of Dilatancy and Permeability in Rock Salt," *Proceedings 3, Workshop Über Kluft-Aquifere, Gekoppelte Prozesse in Geosystemen, Hannover, November 2000.* Bericht No. 60/2000. Eds. O. Koldetz, et al. Hannover, Germany: Federal Institute for Geosciences and Natural Resources. 107-113.

Knowles, M.K., D. Borns, J. Fredrich, D. J. Holcomb, R. Price, D. Zeuch, T. Dale, and R.S. Van Pelt. 1998. "Testing the Disturbed Zone Around a Rigid Inclusion in Salt," *The Mechanical Behavior of Salt, Proceedings of the Fourth Conference, Ecole Polytechnique, Montreal, Quebec, Canada, June 17 and 18, 1996.* Eds. M. Aubertin and H.R. Hardy, Jr. Clausthal-Zellerfeld, Germany: Trans Tech Publications. 175-188.

Knowles, M. K., and C. L. Howard. 1996. "Field and Laboratory Testing of Seal Materials Proposed for the Waste Isolation Pilot Plant," *Waste Management '96, Session 7, Tucson, AZ, February 25-29, 1996.* Tucson, AZ: Laser Optics, Inc. Paper 7-1 (CD-ROM).

Krieg, R.D. 1984. *Reference Stratigraphy and Rock Properties for the Waste Isolation Pilot Plant (WIPP) Project.* SAND83-1908. Albuquerque, NM: Sandia National Laboratories.

Langer, M. 1984. "The Rheological Behavior of Rock Salt," *The Mechanical Behavior of Salt, Proceedings of the First Conference, Pennsylvania State University, Univeresity Park, PA, November 9-11, 1981.* Eds. H.R. Hardy, Jr. and M. Langer. Clausthal-Zellerfeld, Germany: Trans Tech Publications. 201-231.

Mellegard, K.D., and T.W. Pfeifle. 1993. *Creep Tests on Clean and Argillaceous Salt From the Waste Isolation Pilot Plant.* SAND92-7291. Albuquerque, NM: Sandia National Laboratories.

Munson, D.E. 1979. *Preliminary Deformation-Mechanism Map for Salt (With Application to WIPP).* SAND79-0076. Albuquerque, NM: Sandia National Laboratories.

Munson, D.E., and P.R. Dawson. 1984. "Salt Constitutive Modeling Using Mechanism Maps," *The Mechanical Behavior of Salt, Proceedings of the First Conference, Pennsylvania State University, University Park, PA, November 9-11, 1981.* Eds. H.R. Hardy, Jr. and M. Langer. Clausthal-Zellerfeld, Germany: Trans Tech Publications. 717-737.

Park, B.Y. 2002. "Analysis Plan for Structural Evaluation of WIPP Disposal Room Raised to Clay Seam G." Analysis Plan AP-093, Revision 1. Carlsbad, NM: Sandia National Laboratories (On file in the Sandia WIPP Records Center as ERMS# 524805).

Park, B.Y., and J.F. Holland. In review. *Structural Evaluation of WIPP Disposal Room Raised to Clay Seam G*. SAND2003-3409. Carlsbad, NM: Sandia National Laboratories.

Peach, C.J. 1991. "Influence of Deformation on the Fluid Transport of Properties of Salt Rocks." PhD thesis. Geologica Ultraiectina no. 77. Utrecht, The Netherlands: Rijksuniversiteit te Utrecht, Instituut voor Aardwetenschappen.

Pfeifle, T.W., F.D. Hansen, and M.K. Knowles. 1996. "Salt-Saturated Concrete Strength and Permeability," *Materials for the New Millenium, Proceedings of the Fourth Materials Engineering Conference, Washington, D.C., November 10-14, 1996*. Ed. K.P. Chong. New York, NY: American Society of Civil Engineers.

Pfeifle, T.W., N.S. Brodsky, and D.E. Munson. 1998. "Experimental Determination of the Relationship Between Permeability and Microfracture-Induced Damage in Bedded Salt," *Proceedings, 3rd North American Rock Mechanics Symposium, NARMS '98, Cancún, Mexico, June 3-5, 1998*. Published in *International Journal of Rock Mechanics and Mining Sciences & Geomechanics Abstracts*. Vol. 35, no. 4/5, Paper No. 042.

Pfeifle, T.W., and L.D. Hurtado. 1998. "Permeability of Natural Rock Salt From the Waste Isolation Pilot Plant (WIPP) During Damage Evolution and Healing," *Proceedings, 3rd North American Rock Mechanics Symposium, NARMS '98, Cancún, Mexico, June 3-5, 1998*. Published in *International Journal of Rock Mechanics and Mining Sciences & Geomechanics Abstracts*. Vol. 35, no. 4/5, Paper No. 028.

Powers, D.W. 2000. "Core Descriptions from Location 1, S90 Drift, for DRZ Test Program, April 2000, Contractor's Report." Carlsbad, NM: Sandia National Laboratories (Copy on file in the Sandia WIPP Records Center as ERMS #510137).

Powers, D., C.R. Bryan, and D.M. Chapin. 2001. "Laboratory Studies of Salt Cores from the WIPP Disturbed Rock Zone, (January 31, 2001 – July 31, 2001)." "Sandia National Laboratories Technical Baseline Reports, WBS 1.3.5.4." "Repository Investigations, Milestone RI020, July 31, 2001." Carlsbad, NM: Sandia National Laboratories. 7-1 to 7-7. (Copy on file in the Sandia WIPP Records Center as ERMS# 518970).

Repository Isolation Systems Department. 1996. *Waste Isolation Pilot Plant Shaft Sealing System Compliance Submittal Design Report*. SAND96-1326. Albuquerque, NM: Sandia National Laboratories. 2 Vols.

Sandia National Laboratories. 1996a. "DRZ Permeability." Carlsbad, NM: Sandia National Laboratories (Copy on file in the Sandia WIPP Records Center as WPO# 32038).

Sandia National Laboratories. 1996b. "Salado Anhydrite Permeability in the X-Direction." Carlsbad, NM: Sandia National Laboratories (Copy on file in the Sandia WIPP Records Center as WPO# 30603).

Sandia National Laboratories. 1997. "Summary of EPA-Mandated Performance Assessment Verification Test (Replicate 1) and Comparison with the Compliance Certification Application Calculations." Carlsbad, NM: Sandia National Laboratories (Copy on file in the Sandia WIPP Records Center as WPO# 46674).

Senseny, P.E.. 1986. *Triaxial Compression Creep Tests on Salt From the Waste Isolation Pilot Plant.* SAND85-7261. Albuquerque, NM: Sandia National Laboratories.

Spiers, C.J., J.L. Urai, and G.S. Lister. 1988. "The Effect of Brine (Inherent or Added) on Rheology and Deformation Mechanisms in Salt Rock," *The Mechanical Behavior of Salt, Proceedings of the Second Conference, Federal Institute for Geosciences and Natural Resources, Hanover, Federal Republic of Germany, September 24-28, 1984.* Eds. H.R. Hardy, Jr. and M. Langer. Clausthall-Zellerfeld, Germany: Trans Tech Publications. 89-102.

Stein, J.S., and W.P. Zelinski. 2003a. "SNL WIPP Analysis Plan AP-106, Revision 0, Analysis Plan for the Testing of a Proposed BRAGFLO Grid to be used for the Compliance Recertification Application Performance Assessment Calculations." Carlsbad, NM: Sandia National Laboratories (Copy on file in the Sandia WIPP Records Center as ERMS# 525236).

Stein, J., and W.P. Zelinski. 2003b. "Analysis Report for Testing of a Proposed BRAGFLO Grid to be used for the Compliance Recertification Application Performance Assessment Calculations." Carlsbad, NM: Sandia National Laboratories (Copy on file in the Sandia WIPP Records Center as ERMS# 526868).

Stone, C.M. 1997. *Final Disposal Room Structural Response Calculations.* SAND97-0795. Albuquerque, NM: Sandia National Laboratories.

Stormont, J. C. 1990. "Gas Permeability Changes in Rock Salt During Deformation." PhD. dissertation. Tucson, AZ: University of Arizona.

Stormont, J. C., and C. L. Howard. 1986. *Development and Implementation: Test Series B of the Small-Scale Seal Performance Tests.* SAND86-1329. Albuquerque, NM: Sandia National Laboratories.

U.S. Department of Energy. 1996. *Title 40 CFR Part 191 Compliance Certification Application for the Waste Isolation Pilot Plant.* Carlsbad, NM: U.S. Department of Energy, Waste Isolation Pilot Plant, Carlsbad Area Office. Vols. I-XXI.

U.S. Environmental Protection Agency. 1998. "40 CFR Part 194: Criteria for the Certification and Recertification of the Waste Isolation Pilot Plant's Compliance with the Part 191 Disposal Regulations: Certification Decision; Final Rule," *Federal Register.* Vol. 63, no. 95, 27353-27406.

U.S. Environmental Protection Agency. 2002. "Additional Guidance to Clarify the Environmental Protection Agency's (EPA's) Expectations for the Waste Isolation Pilot Plant (WIPP) Compliance Recertification Application (CRA)." Letter from Frank Marcinowski, Director, Radiation Protection Division, U.S. Environmental Protection Agency, Office of Air and Radiation to Dr. Inés Triay, Manager, Carlsbad Field Office, U.S. Department of Energy, dated August 6, 2002. Washington, DC: U.S. Environmental Protection Agency, Office of Air and Radiation.

Van Sambeek, L.L., J.L. Ratigan, and F.D. Hansen. 1993a. "Dilatancy of Rock Salt in Laboratory Tests," *Rock Mechanics in the 1990s, the 34th U.S. Symposium on Rock Mechanics, University of Wisconsin-Madison, USA, June 27-30, 1993*. Ed. B.C. Haimson. *International Journal of Rock Mechanics and Mining Sciences & Geomechanics Absracts*. Vol. 30, no. 7, 735-738.

Van Sambeek, L.L., D.D. Luo, M.S. Lin, W. Ostrowski, and D. Oyenuga. 1993b. *Seal Design Alternatives Study*. SAND92-7340. Albuquerque, NM: Sandia National Laboratories.

Vaughn, P., M. Lord, and R. MacKinnon. 1995. "FEP Screening Issue S-6 Dynamic Alteration of the DRZ/Transition Zone." Carlsbad, NM: Sandia National Laboratories (Copy on file in the Sandia WIPP Records Center as ERMS# 230797).

Wakeley, L.D., and D.M. Walley. 1986. *Development and Field Placement of as Expansive Salt-Saturated Concrete (ESC) for the Waste Isolation Pilot Plant (WIPP)*. Technical Report SL-86-36. Vicksburg, MS: Dept. of the Army, Waterways Experiment Station, Corps of Engineers.

Wakeley, L.D., J.J. Ernzen, B.D. Neeley, and F.D. Hansen. 1994. *Salado Mass Concrete: Mixture Development and Preliminary Characterization*. SAND93-7066. Albuquerque, NM: Sandia National Laboratories.

Wallner, M. 1984. "Analysis of Thermomechanical Problems Related to the Storage of Heat Producing Radioactive Waste in Rock Salt," *The Mechanical Behavior of Salt, Proceedings of the First Conference, Pennsylvania State University, University Park, PA, November 9-11, 1981*. Eds. H.R. Hardy, Jr. and M. Langer. Clausthal-Zellerfeld, Germany: Trans Tech Publications. 738-763.

Wawersik, W.R., and D.W. Hannum. 1979. *Interim Summary of Sandia Creep Experiments on Rock Salt from the WIPP Study Area, Southeastern New Mexico*. SAND79-0115. Albuquerque, NM: Sandia National Laboratories.

Wawersik, W.R., and C.M. Stone. 1989. "A Characterization of Pressure Records in Inelastic Rock Demonstrated by Hydraulic Fracturing Measurements in Salt," *International Journal of Rock Mechanics and Mining Sciences & Geomechanics Abstracts*. Vol. 26, no. 6, 613-627.Wawersik, W.R., L.W. Carlson, J.A. Henfling, D.J. Borns, R.L. Beauheim, C.L. Howard, and R.M. Roberts. 1997. *Hydraulic Fracturing Tests in*

Anhydrite Interbeds in the WIPP, Marker Beds 139 and 140. SAND95-0596. Albuquerque, NM: Sandia National Laboratories.

Wieczorek, K., and U. Zimmer. 1999. "Hydraulic Behavior of the Excavation Disturbed Zone Around Openings in Rock Salt," *Proceedings of the Seventh International Conference on Radioactive Waste Management and Environmental Remediation, ICEM '99, September 26–30, 1999, Nagoya, Japan*. New York, NY: American Society of Mechanical Engineers (CD-ROM).

Appendix A: Salt-Based Concrete

Salt-based concrete constitutes the major engineered material in the Option D panel closure design. Because the behavior of the salt DRZ depends upon interaction with the concrete monolith, characteristics of the salt-based concrete are essential for incorporation into the analyses. Portland cement concrete has exceptionally low permeability and is widely used for hydraulic applications. Salt-based concrete, such as the SMC specified for the Option D closure, is essentially Portland cement concrete with the mixing water saturated with respect to NaCl. Salt-saturated concrete has been used successfully as a seal material in potash and salt mining applications. Salt-based concrete has received less attention than ordinary Portland cement (OPC) concrete, however several specific investigations provide a comparison between salt-based and OPC concrete. Upon hydration, unfractured concrete is nearly impermeable, having a permeability of less than 10^{-20} m^2. From laboratory and field experiments, it has been demonstrated that salt-based concrete possesses engineering properties similar to OPC concrete. And, salt-based concrete is compatible with the salt mine environment.

The following text establishes performance expectations for the SMC used in the Option D panel closure construction. It is included in this document as an appendix to the DRZ discussion, because the analysis necessary for PA involves a system comprising intact salt, damaged salt, and the concrete monolith. Properties of salt-based concrete are established in the laboratory, in scale-model field tests (Section 4.6) and at the full scale (Section 4.9).

Pfeifle et al. (1996) conducted tests on two salt-based concretes: (1) SMC and (2) cured concrete recovered from the shaft plug of an existing salt mine (referred to as MSC concrete). The SMC was specifically designed for use in the WIPP shaft sealing system and was tailored to have limited shrinkage and to be compatible with WIPP salt through the addition of salt to the mixing water (Wakeley et al., 1994). The MSC concrete was originally placed as a shaft plug in a commercial salt mine located near the St. Lawrence seaway and consisted of two types of mixtures, MSC(1) and MSC(2). The MSC(1) concrete comprised a typical 27.6 MPa (4,000 psi) design batch using coarse and fine (sand) aggregates and Type I/II cement. The water for the MSC(1) was mixed with salt in a truck to produce a saturated brine before the solid components were added to the batch. MSC(2) concrete comprised a sand/cement mix that was placed in the shaft by tremie line under 70 meters of water. Granular salt was added to this batch to form brine during mixing.

Table A.1 summarizes the strength and permeability testing conducted on the SMC and MSC cores. Figure A.1 plots permeability as a function of the gas pressure difference applied during the permeability testing of the SMC and MSC specimens as well as ESC specimens, which are described further in the discussion of small-scale seal performance tests (Section 4.6). The permeability of the SMC was typically of the order of 10^{-21} m^2, while the permeability of the MSC was approximately four orders-of-magnitude higher, i.e., 10^{-17} m^2. This difference in permeability was attributed to two factors: (1) the stringent design requirements established to limit fluid flow through the WIPP SMC shaft sealing components and (2) the limited quality control used in the placement of the MSC concrete under extreme conditions (i.e., placement under water). The permeability of the ESC from the SSSPT (Section 4.6) is approximately

$10^{-19}m^2$, which falls between the permeability for the SMC and MSC tests. The strengths of the two types of concrete are comparable, and increase appreciably when confined.

Table A.1 Summary of Strength and Permeability Tests on SMC and MSC Concrete Specimens.

Specimen I.D.	Permeability (m^2)	Confining Pressure (MPa)	Stress Difference At Failure (MPa)	Elastic Modulus, E (GPa)	Poisson's Ratio, ν
Salado Mass Concrete					
40SM4-19/2-1/1	$2\times10^{-21} - 8\times10^{-21}$	0	44.2	36.3	0.19
32SM4-25/1-1/1	–	5	75.8	30.5	0.20
40SM4-11/2-1/1	9×10^{-22}	10	80.5	36.7	0.35
40SM4-2/1-1/1	–	15	111.4	32.2	0.20
MSC Shaft Concrete					
MSC/D-1	$4\times10^{-17} - 10\times10^{-17}$	0	60.2	18.3	0.15
MSC/O-2/2	$2\times10^{-17} - 4\times10^{-17}$	0	45.3	22.6	0.23
MSC/K-2/2	$2\times10^{-17} - 4\times10^{-17}$	0	56.4	32.8	0.17

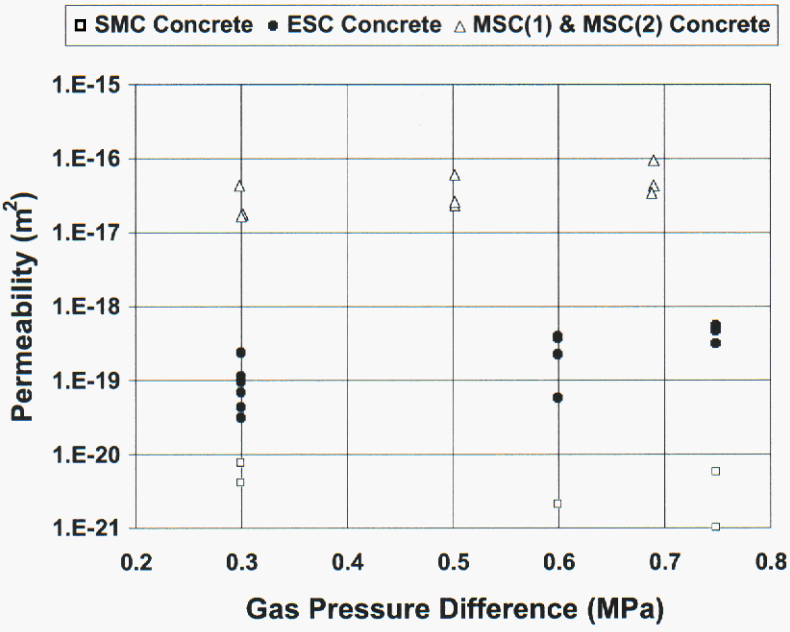

Figure A.1. Permeability of SMC, ESC, and MSC Concrete Specimens Versus Gas Pressure Difference.

The permeability of salt-based concrete was measured in the Small Scale Seal Performance Test (SSSPT) for a decade and corroborated by laboratory measurements. From these tests, values and ranges of concrete permeability have been developed. For PA calculations, permeability of SMC seal components is treated as a sampled variable, for which the probability distribution function is plotted in Figure A.2.

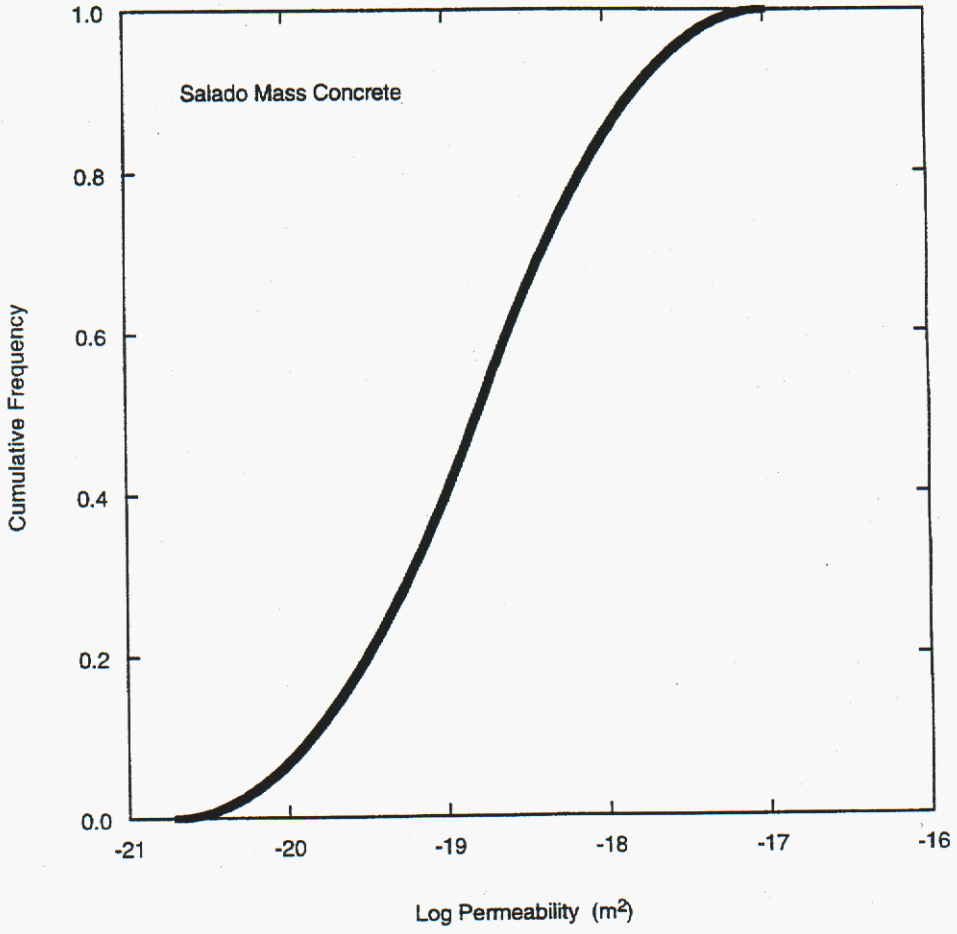

Figure A.2. Cumulative Distribution Function for Permeability of SMC (after Repository Isolation Systems Department, 1996, WIPP Shaft Seal System Compliance Submittal Design Report, Appendix A).

Appendix B: DRZ Issues Addressed in the CCA

The disturbed rock zone was addressed in several compliance documents. Because these references comprise the basis for the EPA compliance determination, a review of the disturbed rock zone discussions as they exist in the compliance record is appropriate. The conceptual model implemented at the time of the compliance submittal has been advanced in certain ways, as discussed in the main paper. Modest research effort has continued in the underground at the repository horizon as well as collaborative research on the international frontier. Based on recent information obtained since the CCA coupled with historical information, the current understanding and description of the DRZ differ somewhat from the concepts put forward in the CCA. A word search on DRZ was conducted for the CCA and supporting documents. The following reference sections of the CCA were examined in preparation of the DRZ discussions in the main text to ensure consistency between the CCA baseline and the current discussions of the DRZ. These documents are identified below and a brief evaluation or summary is provided. Thus, the bases of the DRZ considerations in the CCA have been reviewed in preparation of this memorandum.

The Compliance Application:
Section 2.2.1.3 Hydrology of the Salado: summarizes hydraulic tests in salt and anhydrite. Measured permeabilities are all lower than 10^{-18} m^2. Other discussion acknowledges that flow observations are complex.

Section 3.2 Repository Configuration: states that the panel closure system "will prevent further development of the DRZ in panel entries." When the Option D panel closure is constructed, this statement should be modified to include the fact that the DRZ would be mined out and any existing DRZ would heal shortly thereafter.

Section 3.3.1.3.2 Clay Columns: clay column stiffness is sufficient to heal fractures, thus removing the DRZ.

Section 3.3.1.5.1 DRZ Behavior: discusses DRZ healing as accounted for in the Shaft Seal Design.

Section 3.3.2 Panel Closure System: again notes that the PCS would prevent the existing DRZ from increasing in permeability. Option D would change this position. Also, this section notes that the panel concrete would not degrade to a condition that is more permeable than the DRZ.

Section 6.0.2.2 Undisturbed Performance: presents arguments for DRZ healing around the concrete components. In the absence of elevated pressure in the repository, salt creep would also eventually result in substantial compaction of the waste.

Section 6.4.3.1 Creep Closure: discusses creep closure and development of the porosity surface.

Section 6.4.4 This section discusses the Shaft Seal System (from Appendix SEAL) and its representation in BRAGFLO.

Section 6.4.5 The Salado: discusses modeling interbeds and fracturing.

Section 6.4.5.1 Impure Halite: begins by noting that gas will not flow in halite.

Section 6.4.5.2 Salado Interbeds: identifies the distinct anhydrite interbeds modeled in BRAGFLO (MB 138, MB 139, and anhydrite layers a and b). MB 139 and anhydrite a and b are included within the DRZ. The DRZ is extended to reach MB 138 "because of uncertainty in the extent and properties of the DRZ and the associated long-term isolation of MB 138 from the repository." The extent of the DRZ as modeled in the CCA and PAVT is much larger than practical observation, geophysical measurement, and modeling would suggest.

Section 6.4.5.3 DRZ: states that PA approximates the effects of the DRZ conservatively by extending it from MB138 to MB 139, thus creating a permanent high-permeability region that does not significantly impede flow between the repository and affected interbeds. Table 6-17 lists the DRZ parameter values as discussed in the main CCA text. The DRZ representation has been modified for the re-certification calculations to include Option D closures. Therefore, permeability near the Option D closure has been assigned values consistent with the best available information since the CCA.

Section 6.4.7.1.1 Direct Brine Release During Drilling: presents arbitrarily assumed DRZ for pillars.

Section 6.4.10.1 Disposal System Flow and Transport Modeling (BRAGFLO and NUTS): discusses start-up permeabilities, constant permeabilities and other initial conditions, such as gas reaction rates.

Section 6.5.4 Uncertainty: basically states that PCS and DRZ are assigned permeability of 10^{-15} m^2.

Section 7.2 Monitoring: states that "Monitoring the DRZ hydrologic properties would not provide relevant information of verify assumptions used in PA; therefore, they will not be monitored during the operational period nor during the postclosure period." This statement was presumptuous, as ongoing evaluation of DRZ provides more realistic appreciation of the DRZ than reflected in the CCA.

Section 7.2.3.1 Geomechanical Monitoring Program: countermands the previous statement by acknowledging "...geotechnical measurements will be useful to detect deviations in ...DRZ development.

Section 9.3.1.1 Adequate Models: "concludes that the present DRZ model is adequate to be implemented in performance calculations."

Section 9.3.1.2.2.3 Third Peer Review Panel Concern-Repository Fluid Flow: presented and discussed the issue stated as "Consolidation of the waste, panel seals, and repository disturbed rock zone (DRZ) over time would result in lower permeabilities for these regions." The effects

of dynamic permeability of the DRZ were modeled and "results in computed releases to the accessible environment that are essentially equivalent to the baseline case. In addition, dynamic alteration of the DRZ/TZ has an insignificant effect on waste room conditions relevant to blowout cuttings, and spalling releases."

Section 9.3.1.2.8.3 Third Peer Review Panel Concerns: revisits direct brine release owing to penetration into the DRZ.

Appendices
Appendix SOTERM 7.1.2 Use of Brine End Members: Material here is of no consequence to DRZ considered in the repository horizon.

Appendix SEAL (contains 210 call outs of DRZ): Discussion in Appendix SEAL concerns the shaft seal system. In the design and analysis of the shaft system, the DRZ was incorporated into the analysis in considerable detail. The shaft seal design thoroughly accounted for the DRZ, as noted by the EPA comments found in other sections; however, the DRZ near the disposal rooms is complicated by the horizontal stratigraphy and the size and shape of openings.

Appendix MASS.2.4 CM Development (1982 to Present): The modeling concept for panel closures and an "imperfectly healed DRZ" are noted here.

Appendix MASS.3.1 Darcy's Law: Not applicable for DRZ discussions.

Appendix MASS.13.0 Salado: Flow in the Salado is modeled to occur through interbeds that intersect the DRZ. The conceptual model for Salado fluid flow has primary interactions with three other conceptual models. The interbed fracture conceptual model allows porosity and permeability of the interbeds to increase as a function of pressure.

Appendix MASS Table 1.0 General Modeling Assumptions: Modeling assumptions for various treatment of the DRZ are listed in this table. First, the shaft is surrounded by a DRZ, which heals with time. The DRZ is represented through the permeabilities of the shaft system itself, rather than as a discrete zone. Second, panel closures are modeled with the same properties as the surrounding DRZ. Third, the permeability of the DRZ is constant and higher than intact Salado. Fourth, excavation and waste emplacement result in partial drainage of the DRZ. The treatment of the shaft within the BRAGFLO model will be simplified for purposes of the re-certification PA.

Appendix MASS.13.4 Flow in the Disturbed Rock Zone: Along with Section 6.4.5.3 this text presents the basic treatment of the DRZ in CCA calculations. The conceptual model implemented in the PA uses values for the permeablility and porosity of the DRZ that do not vary with time. A screening analysis examined an alternative conceptual model for the DRZ in which permeability and porosity changed dynamically in response to changes in pressure (Vaughn et al., 1995). The Vaughn et al. report implemented a fracturing model in BRAGFLO for the DRZ. This fracturing model is identical to the existing anhydrite interbed alteration model. They concluded that the DRZ fracture model yielded results "essentially equivalent" to those with the DRZ constant. Treatment of anhydrite fracture and the interplay with the DRZ is

being treated in some detail in the re-certification calculations and changes to the conceptual models for Salado flow were subjected to Peer Review consistent with 40 CFR 194.27 and NUREG-1297.

Appendix PAR 11 Log Intrinsic Permeability—All Clay Shaft Materials: This section discusses how the DRZ permeability was incorporated into the model element for the clay shaft seal component.

Appendix PAR 9 Log Intrinsic Permeability—Asphalt: This section discusses how the DRZ permeability was incorporated into the model element for the asphalt shaft seal component.

Appendix PAR 12 Intrinsic Permeability-Shaft Disturbed Rock Zone: Along with parameters 9 and 11, this discusses *in situ* measurements made on the Air Intake Shaft (Dale and Hurtado, 1998) and in Room D (Knowles and Howard, 1996).

Appendix PAR Tables PAR-2 and PAR-3: These tables are identical and list seal materials and DRZ extent. This information is not applicable to treatment of the DRZ in the repository.

Appendix PAR Tables PAR-6: This table provides permeabilities of various anhydrite layers (MB 139, MB 140 and anhydrite b).

Appendix Peer Conceptual Models: Section 3.7 Disturbed Rock Zone. As noted in the text (Section 2.3) the updated treatment of the DRZ comprised a portion of the independent peer review process.

Technical Support Documents
TSD 23 Section 1.3.24 Disturbed Rock Zone Conceptual Model: here the EPA was not satisfied with DOE's assumption that the permeability of the DRZ remained constant with time. Consequently, this parameter was treated as a variable in the EPA mandated PA verification test.

TSD 23 Section 3.3 198 DRZ_1-PRMX_LOG:DRZ Permeability

Compliance Application Review Documents
CARD 23 Section 4.4.9.1 DOE's Implementation of the Salado Interbeds Conceptual Model in CCA

CARD 23 Section 1.3.25.1 DOE's Model Description

CARD 23 Table 2.3.1 Alternative CM's Seriously Considered for PA

CARD 23 Section 4.4.7.1 DOE's Implementation of the Salado Conceptual Model into CCA

CARD 23 Section 4.4.11 Shaft and Shaft Seal CM

CARD 23 Section 4.4.12 Disturbed Rock Zone (DRZ) Conceptual Model

CARD 23 Section 7.3.2.3 Salado CM
CARD 14 Section 14.B.4 DOE Methodology and Conclusions, Rustler, Dewey Lake, and Santa Rosa Formation Hydrology

CARD 14 Section 14.E.4 DOE Methodology and Conclusions

CARD 14 Section 14.E.5 EPA Compliance Review

PAVT
WPO#46674 Rev. 1. Summary of EPA Mandated PAVT

Federal Agencies

US Department of Energy (1)
Office of Civilian Radioactive Waste Mgmt.
Attn: Deputy Director, RW-2
Forrestal Building
Washington, DC 20585

US Department of Energy (7)
Carlsbad Field Office
Attn: I. Triay
G. Basabilvazo
S. Casey
D. Mercer
R. Nelson
R. Patterson
Mailroom
P.O. Box 3090
Carlsbad, NM 88221-3090

US Department of Energy
Office of Environmental Restoration and
Waste Management
Attn: P. Bubar, EM-20
Forrestal Building
Washington, DC 20585-0002

US Department of Energy
Office of Environmental Restoration and
Waste Management
Attn: Mary Bisesi/Lynne Smith, EM-23
Washington, DC 20585-0002

US Environmental Protection Agency (1)
Radiation Protection Programs
Attn: B. Forinash
ANR-460
Washington, DC 20460

Boards

Defense Nuclear Facilities Safety Board
Attn: D. Winters
625 Indiana Ave. NW, Suite 700
Washington, DC 20004

State Agencies

Attorney General of New Mexico
P.O. Drawer 1508
Santa Fe, NM 87504-1508

Environmental Evaluation Group (2)
Attn: Library
7007 Wyoming NE
Suite F-2
Albuquerque, NM 87109

NM Environment Department (1)
Secretary of the Environment
1190 St. Francis Drive
Santa Fe, NM 87503-0968

NM Bureau of Geology & Mineral
Resources
801 Leroy Place
Socorro, NM 87801

Laboratories/Corporations

Battelle Pacific Northwest Laboratories
Battelle Blvd.
Richland, WA 99352

Los Alamos National Laboratory
Attn: B. Erdal, INC-12
P.O. Box 1663
Los Alamos, NM 87544

Washington TRU Solutions (3)
Attn: Library, GSA-214
P.O. Box 2078
Carlsbad, NM 88221

National Academy of Sciences
WIPP Panel

National Academies
Attn: Barbara Pastina (1)
Committee on WIPP
Board on Radioactive Waste Management
500 Fifth Ave NW; Keck 634
Washington, DC 20001

Universities

University of New Mexico
Geology Department
Attn: Library
141 Northrop Hall
Albuquerque, NM 87131

Libraries

Government Information Department
Zimmerman Library
MSC05 3020
University of New Mexico
Albuquerque, NM 87131-0001

New Mexico Junior College
Pannell Library
Attn: Earl Dye
5317 Lovington Highway
Hobbs, NM 88240

New Mexico State Library
Attn: L. Canepa
1209 Camino Carlos Rey
Santa Fe, NM 87507

New Mexico Tech
Joseph R. Skeen Library
801 Leroy Place
Socorro, NM 87801

Foreign Addresses

Francois Chenevier (2)
ANDRA
Parc de la Croix Blanche
1-7 rue Jean Monnet
92298 Chatenay-Malabry Cedex
FRANCE

Commissariat a L'Energie Atomique
Attn: D. Alexandre
Centre d'Etudes de Cadarache
13108 Saint Paul Lez Durance Cedex
FRANCE

Bundesanstalt fur Geowissenschaften und
Rohstoffe
Attn: M. Wallner
Postfach 510 153
D-30631 Hannover
GERMANY

Bundesministerium fur Forschung und
Technologie
Postfach 200 706
5300 Bonn 2
GERMANY

Gesellschaft fur Anlagen und
Reaktorsicherheit
(GRS)
Attn: B. Baltes
Schwertnergasse 1
D-50667 Cologne
GERMANY

Dr.-Ing. Klaus Kuhn
TU Clausthal Institut fur Bergbau
Erzstr. 20
D-38678 Clausthal-Zellerfeld
GERMANY

Dr. Susumu Muraoka
Nuclear Material Control Center
Tokai-Mura, Ibaraki-Ken, 319-11
JAPAN

Nationale Genossenschaft fur die Lagerung
Radioaktiver Abfalle (2)
Attn: NAGRA Library
Hardstrasse 73
CH-5430 Wettingen
SWITZERLAND

AEA Technology
Attn: W. R. Rodwell
424-4 Harwell
Didcot, Oxfordshire OX11 OQJ
UNITED KINGDOM

Internal

MS	Org.	
0701	6100	P. B. Davies
0731	6800	823 Library (2)
0771	6800	D. Berry
1395	6820	P. E. Shoemaker
1395	6821	D. Kessel
1395	6822	M. Rigali
1395	6820	F. Hansen (4)
1395	6820	WIPP Library (10)
9018	8945-1	Central Technical Files
0899	9616	Technical Library (2)